Tribology International 154 (2021) 106749

Contents lists available at ScienceDirect

Tribology International

journal homepage: http://www.elsevier.com/locate/triboint

Review

Directional interfacial motion of liquids: Fundamentals, evaluations, and manipulation strategies

Qingwen Dai [a], Wei Huang [a], Xiaolei Wang [a], M.M. Khonsari [b,*]

[a] National Key Laboratory of Science and Technology on Helicopter Transmission, Nanjing University of Aeronautics and Astronautics, Nanjing, 210016, China
[b] Department of Mechanical and Industrial Engineering, Louisiana State University, 3283 Patrick Taylor Hall, Baton Rouge, LA, 70803, USA

ARTICLE INFO

Keywords:
Directional interfacial motion
Thermocapillary
Surface and interface
Microstructures

ABSTRACT

The Marangoni effect—often invoked to describe the so-called "tears of wine"—is in essence the mass transfer along an interface between two fluids due to a gradient of the surface tension. If, in addition, the system experiences a temperature dependence, the phenomenon is called thermocapillary migration. It is an interfacial phenomenon where chemistry, physics, and engineering intersect and has extensive application prospects in modern machinery. It can accelerate the spreading of liquids to enhance the condensation and heat transfer efficiency in condensation assemblies, contribute to the flow rate in open microfluidics, or manipulate tiny amounts of liquids in microelectromechanical systems. In tribo-systems, although lubricant migration contributes to wet rubbing surfaces, an unexpected migration might disrupt the flow, either partially or fully starve the contact area, and cause system failure. It is important not to inadvertently control the lubricants migration for advancing the design philosophy of modern mechanical components. Hence, this paper presents a comparative review of the fundamentals of interfacial motion of liquids, evaluation methodologies, and manipulation strategies in design. Of particular interest is the implementation of manipulation strategies for modern tribo-systems exposed to thermal gradients and establish general guidelines for the design of miniature rolling bearings, microfluidics, and condensation and heat-transfer devices.

1. Introduction

The Marangoni effect—often invoked to describe the so-called "tears of wine"—was first reported in the 1860s by the Italian physicist Carlo Giuseppe Matteo Marangoni [1–7]. It describes a phenomenon that when the wine is poured into a clean wine glass, it tends to wet the glass wall and form a wine film. Then the generated droplets run down along the glass surface to form a necklace, like tears, as shown in Fig. 1. Fundamentally, this interfacial phenomenon is a mass transfer containing a sequence of surface force events of wetting, capillarity, film instability, and film dynamics. Surface tension gradient along the liquid/gas interface induced by the evaporation of alcohol is the dominant force within the entire process [8–12].

In addition to the aforementioned evaporation-induced surface tension gradient of liquids, there are other mechanisms that can drive liquids moving on solid surfaces without any external forces. A similar interfacial phenomenon triggered by temperature dependence is known as thermocapillary migration (or motion or creep or convection) [13]. It is an intriguing interfacial phenomenon where chemistry, physics, and engineering intersect and has extensive application prospects in modern machinery. For instance, it can accelerate the spreading of liquids to enhance the condensation and heat transfer efficiency in condensation assemblies, contribute to the flow rate in open microfluidics, or manipulate tiny amounts of liquids in microelectromechanical systems (MEMS) [14–16].

Special attention should be paid to the migration encountered in tribo-systems, where thermal gradients are presented due to the proximity of either an external heat source or an internal frictional heat [17–21]. On the one hand, migration could contribute to the wetting of liquid lubricants on rubbing surfaces. On the other hand, however, an unexpected migration might disrupt the flow, starve the contact area, either partially or fully, and cause lubrication failure [22–25]. This is a major concern particularly in spacecraft mechanisms exposed to considerable temperature swings (−150 to 150 °C) that challenge the adoption of liquid lubricants. In general, large thermal gradients in many vital mechanical components such as rolling and sliding bearings require a timely supply of lubricant to the ball tracks on the races to counterbalance the migration-induced lubricant loss that negatively

* Corresponding author.
E-mail address: knonsari@lsu.edu (M.M. Khonsari).

https://doi.org/10.1016/j.triboint.2020.106749
Received 14 September 2020; Received in revised form 19 October 2020; Accepted 26 October 2020
Available online 27 October 2020

affects tribological performance and the machines' service life.

Hence, it is important not to inadvertently control the lubricant's migration for advancing the design philosophy of modern mechanical components. Researchers are continuously trying to manipulate the migration of liquid lubricants to maintain reliability and steadily lubrication conditions. To achieve this goal, the physical mechanisms of thermocapillary migration must be well understood so that one could come up with appropriate design manipulation strategies. A review of the volumes of published papers in the open literature, as summarized in Fig. 2, indicates that abundant theoretical and experimental works have been carried out in this research field over the past decades, with manipulation strategy being the highest area of concentration.

This paper presents a comparative review of the fundamentals of thermocapillary migration, evaluation methodologies, and manipulation strategies in design. Of particular interest is the implementation of anti-migration strategies for modern tribo-systems exposed to thermal gradients and establish general guidelines for the design of miniature rolling bearings, microfluidics, and condensation and heat-transfer devices.

2. Fundamentals

2.1. Migration phenomenon

Fote et al. [26] and Kannel et al. [27] earlier reported that a liquid lubricant tends to creep away from the ball-race interfaces of bearings in the presence of a unidirectional thermal gradient, while it would not creep against the thermal gradient. Researchers have further confirmed that liquid lubricants could also migrate easily on a solid surface in a vacuum environment, and the atmospheric pressure has limited influences on the thermocapillary migration of liquid lubricants, as shown in Fig. 3 [27,28]. This finding is of great importance since constructing a vacuum environment is very time-consuming for multiple experimental explorations.

Furthermore, complexities associated with various types of thermal gradients may exist that requires careful examination of their migration behavior. As an example, when a solid surface is exposed to an omnidirectional thermal gradient, liquid lubricants would migrate to the surrounding simultaneously, forming a ring-like migration configuration. Fig. 4a and Fig. 4b exhibit the migration phenomena of droplets under the unidirectional and omnidirectional thermal gradients, respectively [13,29].

2.2. Basic mechanism

Naturally, a liquid droplet placed on a solid surface can be regarded as a system in which the gas, the liquid and the solid phases coexist. The relationship between three interfacial tensions and contact angle (θ) satisfies Young's equation [30]:

$$\gamma_{SG} = \gamma_{SL} + \gamma \cos\theta \tag{1}$$

where γ (or γ_{LG}), γ_{SL} and γ_{SG} represent the liquid/gas, solid/liquid and solid/gas interfacial tensions, respectively. Typically, the surface tension of liquid decreases with increasing temperature; this variation tendency can be written as:

$$\gamma(T) = \gamma_0 - \gamma_T(T - T_0) \tag{2}$$

where $\gamma(T)$ and γ_0 represent the interface tension at the temperature T and reference temperature T_0, respectively, and γ_T represents the interface tension-temperature coefficient.

At the macro level. As shown in Fig. 5a, for a droplet placed on a non-isothermal solid surface, a tangential force would be generated as a consequence of variations in the surface tension γ along the free surface of the droplet; that is, $\gamma_{Bi} < \gamma_{Fi}$, where the subscript $_B$ and $_F$ represent the front and back edges, and $i = 1, 2, 3, \cdots n$, then Marangoni flow occurs, yielding locomotion from the warm to the cold region. Note that even if the surface is ideally smooth, as the migration progresses, the advancing contact angle exceeds the receding one, causing an asymmetric profile (Fig. 5b). This curvature difference generates a pressure difference across the droplet, producing a capillary flow that opposes the Marangoni flow. Thus, the surface tension gradient has to overcome the capillary effect to initiate the locomotion [31].

At the molecular level. The well-known thermophoresis, or Soret effect — the phenomenon associated with the drifting of molecules along thermal gradients — would also contribute to the migration. As a liquid droplet is exposed to a thermal gradient, the molecules tend to move to the cold side, enhancing the migration [32–34].

2.3. Different solids and lubricants

Investigations reported by Khonsari and Fusaro [35,36], Jones et al. [37], Zaretsky [38], and Wang et al. [39] revealed that increasing the viscosity or surface tension of liquids or decreasing the thermal gradient can weaken the migration behavior to some extent. Dai et al. [40] carried out a systematic study to gain insight into the migration capacity of different lubricants on different surfaces. They tested non-polar lubricants made of synthetic polyalphaolefin (PAO), diester and paraffin oil, polar lubricants of synthetic polyethyleneglycol (PEG) and ionic liquids (IL); metallic solids of gold (Au) and titanium (Ti), non-metallic solids of silicon (Si), high-molecular polymer of polytetrafluoroethylene (PTFE), and their migration performances under a unidirectional thermal

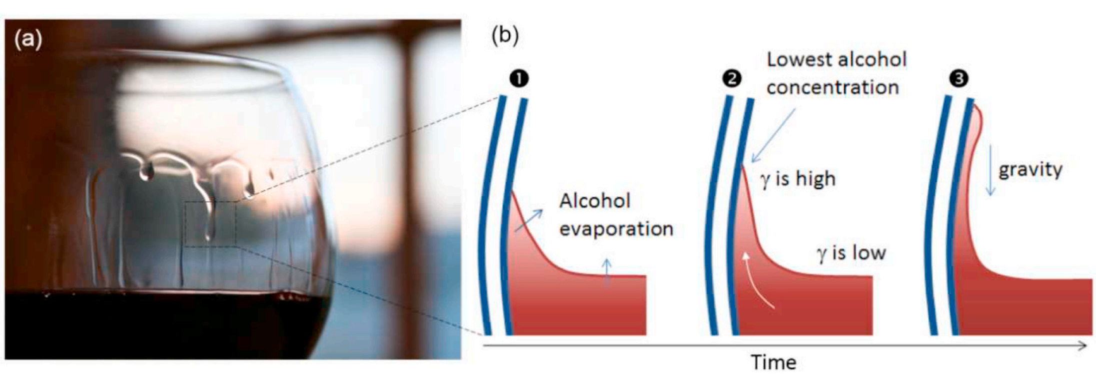

Fig. 1. (a) Tears of wine form on a wine glass. (b) ❶ Wine containing alcohol continuously evaporates from the surface at a rate higher than water, and the alcohol concentration decreases faster in the meniscus due to its higher surface area in relation to its small volume. ❷ This causes a surface tension (γ) gradient that moves the meniscus up the walls of the glass. As the meniscus begins to form a film on the surface of the glass' walls, it gets even more depleted of alcohol, which in turn causes a larger surface tension gradient. ❸ More wine gets pulled up the walls of the glass until droplets form, then gravity takes effect and tears of wine run down the sides of the glass and back into the bulk of the wine [4].

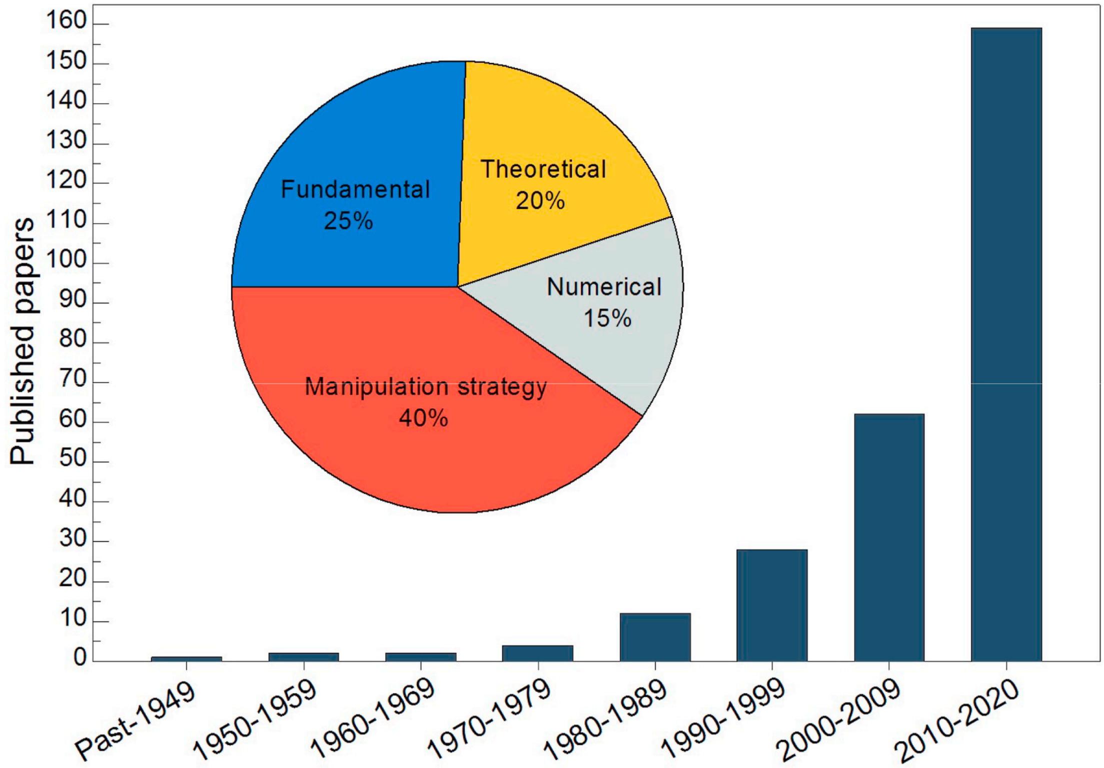

Fig. 2. Related investigations on the thermocapillary migration of liquids.

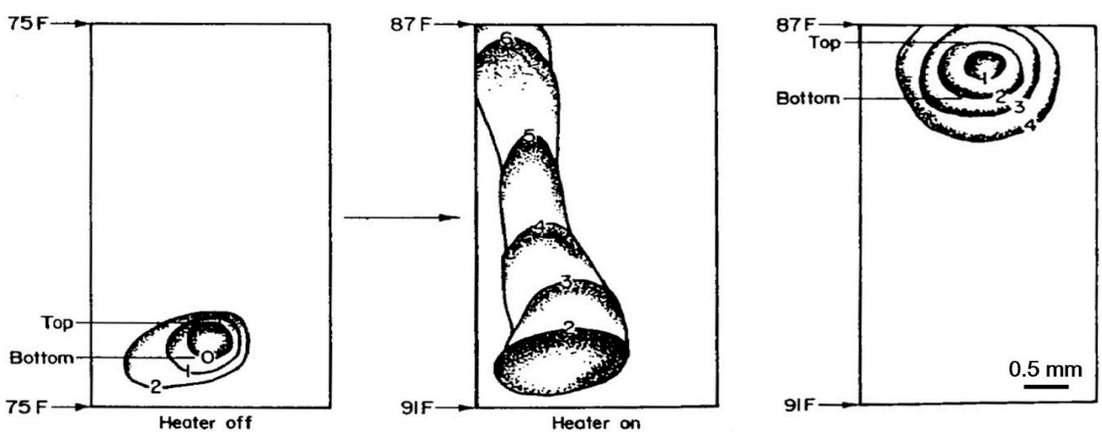

Fig. 3. Migration phenomenon of a KG-80 droplet on a steel plate under a unidirectional thermal gradient of ~1.3 °C/mm in a 10 mPa vacuum chamber [27].

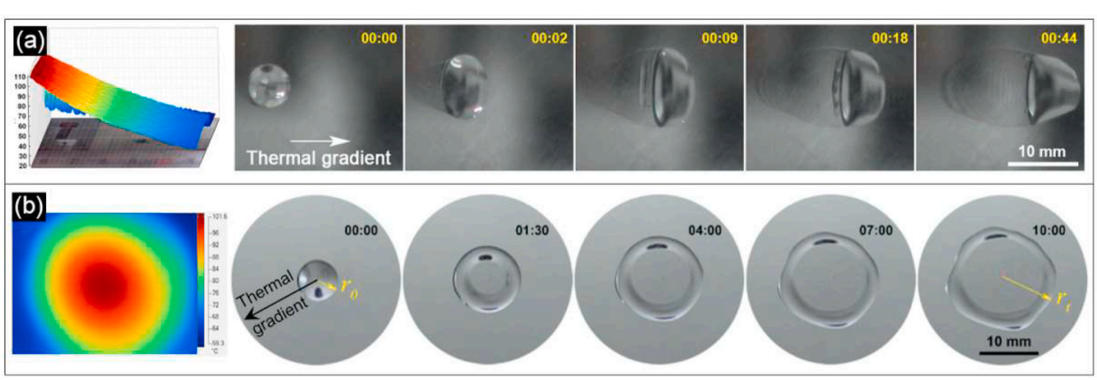

Fig. 4. Migration phenomena of droplets on a steel plate under the (b) unidirectional [13] and (c) omnidirectional [29] thermal gradient of ~3 °C/mm in a normal environment.

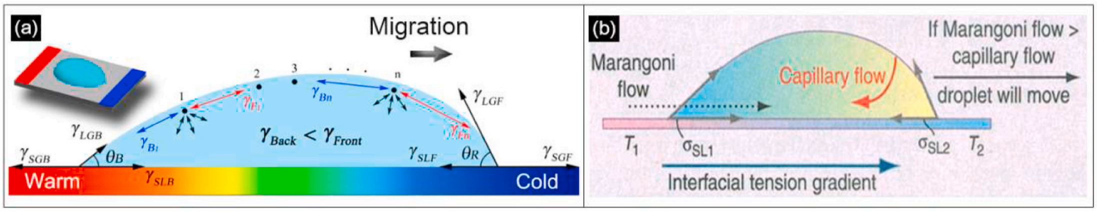

Fig. 5. (a) Thermocapillary migration mechanism. (b) Flow patterns inside the droplet and on the liquid/solid interface due to the surface tension gradient and capillary pressure [31].

gradient of 2.2 °C/mm are shown in Fig. 6. It is confirmed that non-metallic solids with low surface tension such as PTFE, polar lubricants such as PEG or ILs, all have a strong anti-migration capacity [41]. These results provide basic knowledge for the design of tribological components with thermal gradients.

2.4. Solids impregnated with lubricants layers

Thermocapillary migration of droplets on solids impregnated with lubricant layers is different from that on dry ones [42–44]. Quere et al. [45] found that migration can be markedly enhanced when using lubricant-impregnated surfaces as compared to those with solid substrates. Results shown in Fig. 7a and Fig. 7b show that migration can increase at least 5-fold quicker under a thermal gradient of 2 °C/mm. Kumar et al. [46] pointed out that a water droplet placed on a thin lubricant layer of fluorocarbon could transform from lens-shaped to spherical shape as the dosage increases from 4 to 17 μL. More interestingly, the examination of the thermocapillary migration of droplets on free surfaces with immiscible liquids revealed that the lens-shaped drops move from warm toward cool regions while spherical drops move in the opposite direction, as shown in Fig. 7c and d. This dual behavior can be understood via analyzing the surface deformation and velocity profiles of thin lubricant layers subject to a lateral thermal gradient. Lubricant layers allow thermocapillary transport of drops with higher migration speeds than solid substrates and lower internal temperature fluctuation.

Physically, when solid surfaces are impregnated with lubricants, the pinning effect [47] at the vicinity of the three-phase contact line could be weakened significantly, accommodating the locomotion of droplets to occur easily. The front edge of a droplet wets while the back edge de-wets the solid surface as the migration progresses due to the contact angle hysteresis effect. Impregnating the solid surfaces with liquid lubricants can minimize the contact angle hysteresis effect, contributing to the migration.

2.5. Internal flow visualization

Visualization of the internal micro-flows has recently found growing interest. The most popular instrument adopted for this purpose is the micro-particle image velocimetry (μ-PIV) system [48–51]. Fig. 8a shows the in-situ observation on the thermocapillary convection in sessile droplets by Zhao et al. [52]. Two vortices due to Marangoni convection can be seen inside the droplet. Via the confocal μ-PIV technique, Pradhan et al. [53] presented a clear view inside the thermocapillary convection of a stationary sessile water droplet on a horizontal surface with an imposed thermal gradient, and liquid flows from hot side to cold side along the apex of droplet while inside flows from the cold side to the hot side, forming thermocapillary convection (Fig. 8b). Yoda et al. [54] demonstrated how thermal convection could occur inside a liquid film subjected to a thermal gradient. Similarly, two internal vortices are generated at the cooled and heated sides (Fig. 8c). Although PIV technique could provide clear insights into the inner flow vortex, for liquids with complex morphologies, the flow fields remain uncovered and difficult to observe [55].

There are many types of thermocapillary flows — e.g., binary droplets [56], droplets in another immiscible liquid [57,58], liquid films [59–62], liquid marbles [63,64], and bubbles [65] — with varying

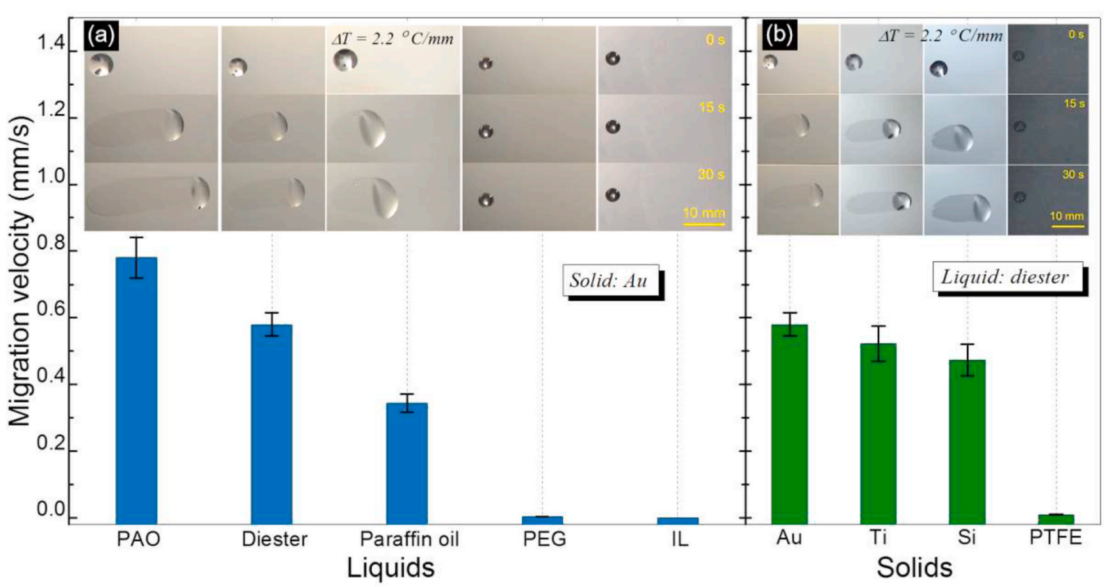

Fig. 6. Migration phenomena and velocities: (a) different lubricants of synthetic polyalphaolefin (PAO), diester, paraffin oil, synthetic polyethyleneglycol (PEG), and ionic liquids (IL) on the Au surface and (b) diester droplets on different surfaces of gold (Au), titanium (Ti), silicon (Si), and polytetrafluoroethylene (PTFE) [40]. (For interpretation of the references to colour in this figure legend, the reader is referred to the Web version of this article.)

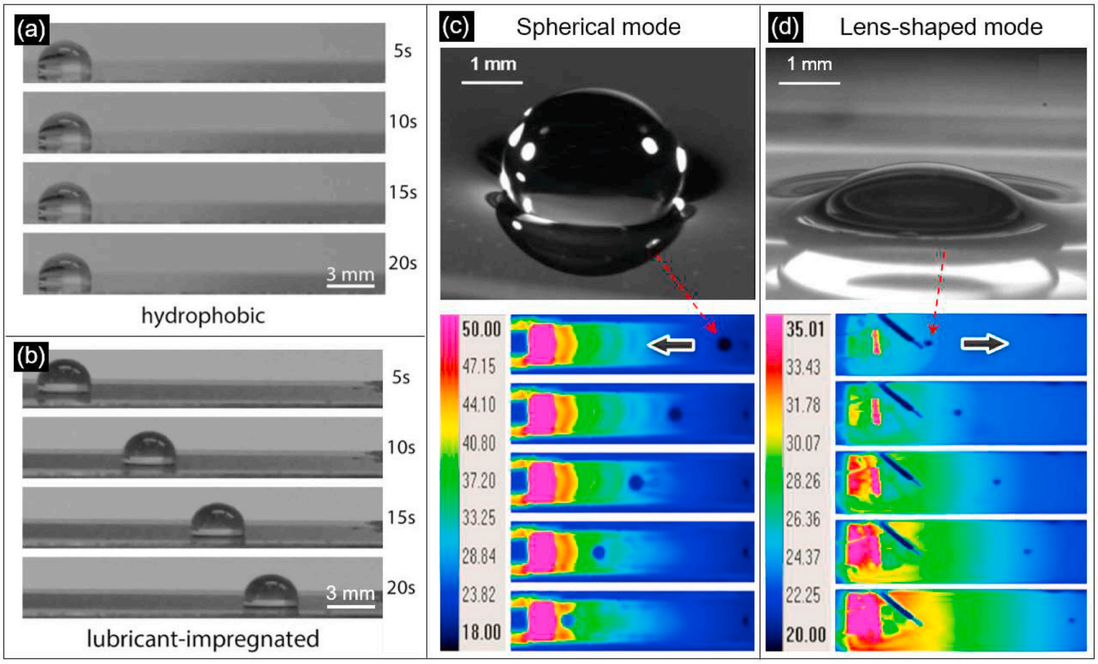

Fig. 7. Chronophotograph of 10 μL water drops exposed to a thermal gradient of 1.8 °C/mm on a (a) smooth hydrophobic surface and (b) smooth hydrophobic surface impregnated with silicone oil (7.5 mPa s) [45]. (c) A spherical droplet (17 μL, 3.2 mm diameter) and (d) lens-shape droplet (4 μL, 2 mm diameter) resting on a thin lubricant layer of fluorocarbon (FC-43), and the corresponding characteristics of thermocapillary migration of (c) spherical mode toward the source of heat (~0.9 °C/mm) and (d) lens-shaped mode away from the heat source (~0.55 °C/mm) [46].

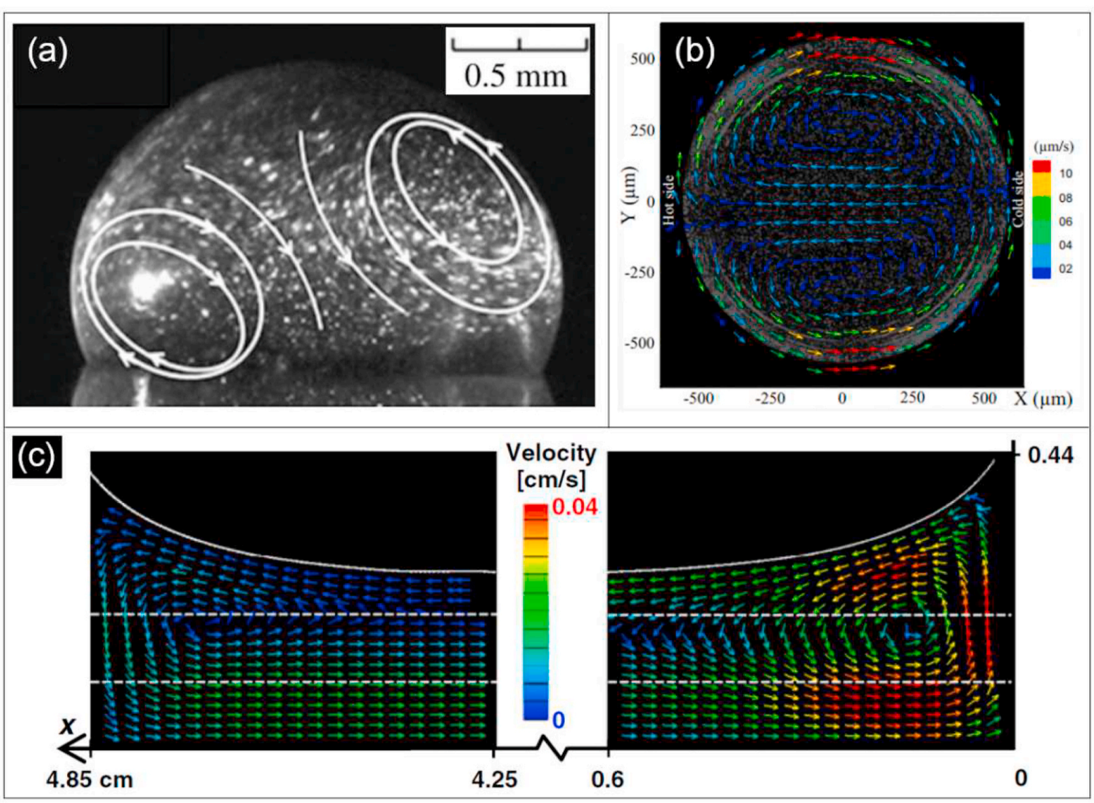

Fig. 8. (a) PIV images of the bulk liquid in the droplet of two vortices due to Marangoni convection [52]. (b) Top view on the velocity vector field inside a droplet at Z = 50 μm from the substrate surface. (c) Side view on the velocity vector field inside a liquid film at the cooled and heated sides [54].

Table 1
Research progresses of analytical models for evaluating the thermocapillary migration performances.

Thermal gradients	Solids	Configuration	Additional conditions	References
Unidirectional	Horizontal	Thin film	Most and complete wetting	Brochard [83]
			Complete wetting	Wasan et al. [31]
			Contact angle hysteresis effect	Troiana et al. [84], Dai et al. [85]
			Viscosity-temperature effect	Wang et al. [13]
			Structured solid surfaces	Karapetsas et al. [86]
			Structured solid surfaces, viscosity-temperature effect	Dai et al. [87], Bai et al. [88]
			Buoyancy effect, density-temperature effect	Hu et al. [89]
		Spherical cap	Contact angle hysteresis effect	Brochard et al. [90]
			Dynamic contact line	Smith et al. [91], Davis et al. [92–95]
			Oscillatory solid surfaces, contact angle hysteresis effect	Chaudhury et al. [96,97]
			Solid surfaces with liquid layers	Quere et al. [45]
			Molecular and gravitational forces	Intyre et al. [98]
		Spherical cap and lens	Solid surfaces with liquid layers	Kumar et al. [46]
		Arbitrary shape	Dynamic contact line	Ford et al. [99]
		Sphere	Reduced gravity	Subramanian et al. [100–102]
	Inclined	Spherical cap	Solid surfaces with liquid layers	Mamalis et al. [103]
			Dynamics contact line	Karapetsas et al. [104]
		Thin film	Varying inclination angle	Khonsari et al. [105]
Omnidirectional	Horizontal	Thin film	Viscosity-temperature effect	Wang et al. [29]
Unidirectional	Horizontal	Spherical	Varying geometric dimensions	Subramanian et al. [106]

Note: In the column of additional conditions: default constant viscosity, thermal gradient, and contact angle are used unless specified.

degrees of complexity. However, the fundamental mechanisms of these thermal flows are the same: they are all manifestation of surface tension gradient induced by thermal unbalance. These experimental investigations provide clear insights into the thermocapillary migration and deeply advance the understanding of the interfacial phenomenon.

3. Evaluations

3.1. Analytical models

Rich volumes of analytical research papers on thermocapillary migration have appeared over the past decades [66–82]. Table 1 provides a succinct summary of the relevant papers with appropriate discussions that follow in the next section.

3.1.1. Geometrical morphology

Originally, Greenspan [107] established a theoretical model for the movement of a small viscous droplet on a smooth solid surface in which the dynamic contact angle was employed to describe the thermally-induced driving force on droplets. The study revealed that when the thickness of liquid droplets is small enough, the migration can be regarded as a quasi-steady process, and the so-called thin-film lubrication approximate theory holds. This theory can be applied to establish the force balance acting on the liquid film and simplify the fluid mechanical analysis process.

Inspired by this approach, Brochard et al. [83,90] considered three specified wetting conditions of partial wetting (spherical cap, Fig. 9a), most wetting (a thick pancake, Fig. 9a②), and complete wetting (a very thin pancake, Fig. 9a③). As a migration progresses, the thermal gradient induced interfacial tension force becomes the dominated driving force (F_T) acting on the liquid, which is balanced by the fluid viscous resistance force (F_V). By assuming a constant thermal gradient ($C_T = \frac{\partial T}{\partial x} =$ Const) on the solid surface, ignoring the capillary pressure, Brochard et al. arrived at the following a theoretical expression for the migration velocity (U):

$$U = c_0 \frac{h_0}{\mu}\left[\frac{\partial}{\partial x}(\gamma_{SG} - \gamma_{SL}) + \frac{\partial}{\partial T}(\gamma_{SG} - \gamma_{SL})C_T + \frac{1}{2}\gamma_T C_T\right] \tag{3}$$

where h_0 is the height of the liquid film and μ is the liquid dynamic viscosity. The value of the pre-factor c_0 depends on these specific 2-D geometries distinguished by these different wetting conditions. In fact, when the surface is completely wetted by liquid film; that is, the contact angle of 0°, combining Eq. (1), a simplified theoretical expression of the migration velocity (U) can be written as [2,31,108]:

$$U \approx \frac{h_0}{2\mu}\gamma_T C_T \tag{4}$$

This equation provides a quick, at-a-glance view of the influence factors on the migration capacity. It suggests that increasing the liquid viscosity, decreasing the thermal gradient, interface tension coefficient, or the droplet height, could all weaken the migration behavior.

Ford et al. [99] further established a model for a droplet with an arbitrary height profile on a surface imposed with a uniform temperature gradient, as shown in Fig. 9b. By taking the slip boundary condition into consideration; that is, allowing for a slip in the vicinity of the contact lines, they arrived at the following expression for the migration velocity of a 2D droplet:

$$U = \frac{\gamma_T C_T b}{2\mu} - \frac{\gamma_T C_T}{6\mu J} - \frac{\gamma_B \cos\theta_B - \gamma_A \cos\theta_A}{6\mu J L} \tag{5}$$

where $J = \frac{1}{2L}\int_{-L}^{L}\frac{1}{h(x)+3b}dx$, and the θ_B and θ_A denote the contact angles at left and right (Fig. 9b), respectively. The migration velocity can be calculated by determining the value of the integral J with the given height profile and the slip length b.

3.1.2. Contact angle hysteresis effect

The above-mentioned investigations on the migration of droplets with different geometrical shapes are primarily concerned with the influence of the morphology of the problem. Since practically most "smooth-looking" solids are actually rough at the micro or nanometer scale, as the migration progresses, the front edge of a droplet wets while the back edge de-wets the solid surface. The wetting and de-wetting processes could involve the contact angle hysteresis effect [109,110], which yields a variation in the contact angles and affects the migration performance. Chen [84] established a model describing the steady thermocapillary migration of a two-dimensional droplet of a spherical cap taking the contact angle hysteresis effect into account and developed the following expression for the theoretical velocity:

$$U = \frac{1}{6\mu L J}\left[\int_{-L}^{L}\frac{C_T\gamma_T h(x)}{2h(x)+6b}dx - (\gamma_R \cos\theta_R - \gamma_A \cos\theta_A)\right] \tag{6}$$

where J is the same as that in Eq. (5), the θ_R and θ_A denote the advancing and receding contact angles, respectively.

Contact angle hysteresis effect could also introduce a lateral reten-

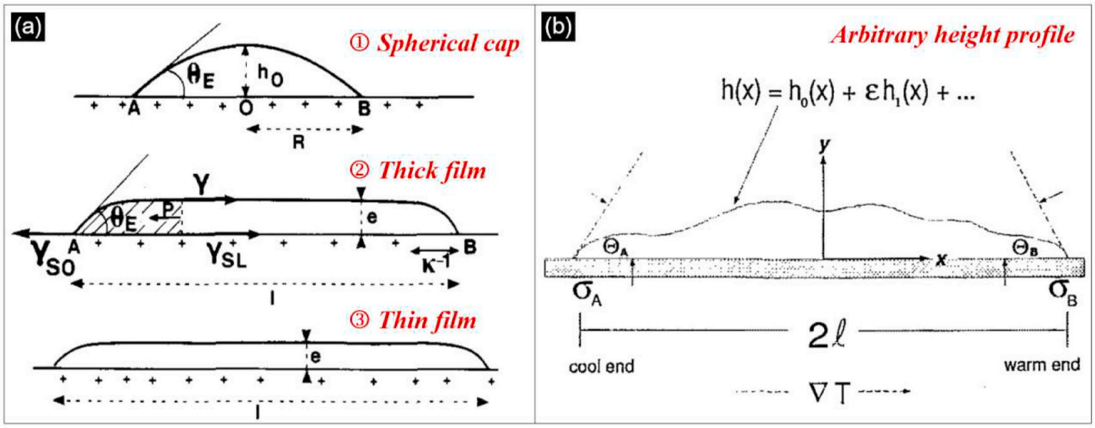

Fig. 9. Droplets with different sections of **(a)** spherical cap, **(a②)** thick pancake, and **(a③)** a thin pancake in the two-dimensional (2-D) case [83]. **(b)** Side view of an infinite 2-D droplet attached to a solid surface with a constant thermal gradient [99].

tion force [111–113], disequilibrating the force balance in the vicinity of the triple-phase contact line on both sides of the droplet. When encountered with a thermal gradient, the thermal gradient induced driving force must overcome the lateral retention force before the droplet can move. Taking this into consideration, Dai et al. [85] revised the theoretical expression for liquid droplets with a thick pancake (Fig. 10) and derived an expression for migration velocity of the following form:

$$U = \frac{(1 + 2\cos\theta)C_T\gamma_T L - 2\gamma_x(\cos\theta_R - \cos\theta_A)}{6\mu L}h \tag{7}$$

Dai et al. experimentally verified the validity of Eq. (7) with surfaces possessing different magnitudes of the contact angle hysteresis effect.

3.1.3. Viscosity-temperature effect

Among most of the reported theoretical contributions, the liquid viscosity is regarded as a constants value in the derivation process. In reality, not only will thermal gradients change the interfacial tension of a liquid can cause migration, but also affect the viscosity of the liquid. In general, the viscosity of a liquid drops exponentially with the increase in temperature as described by Eq. (8),

$$\mu(T) = \mu_0 e^{-b[T - T_0]} \tag{8}$$

where μ_0 and $\mu(T)$ represent the viscosity at reference temperatures T_0 and T respectively, b represents the viscosity-temperature coefficient.

For the migrated droplets in a thin-film shape, the time taken for the temperature to stabilize is shorter than that required for the droplet to move an appreciable distance from the previous location. This implies that the temperature of the droplets will be in equilibrium with that of the substrate surface; that is, $T = T_{Start} - C_T x$ where T_{Start} represents the temperature of the starting position and x denotes the central position of the migrated droplet. Dai et al. [13] took this viscosity-temperature relationship into the theoretical derivation for droplets in a thin-film shape and proposed an effective approach for estimating the thermo-capillary migration velocity:

$$U = \frac{1}{g(x_A, x_R)}\frac{(1 + 2\cos\theta)\gamma_T C_T L}{6\mu_0}h \tag{9}$$

where $g(x_A, x_R) = \frac{1}{bC_T}\left[e^{b(C_T x_A - T_{Start} + T_0)} - e^{b(C_T x_R - T_{Start} + T_0)}\right]$.

Dai et al. reported that substituting the measured height (h) of the liquid film during the migration process into the Eq. (9) could yield a more accurate result, making the theoretical prediction more realistic when compared with experimental measurements.

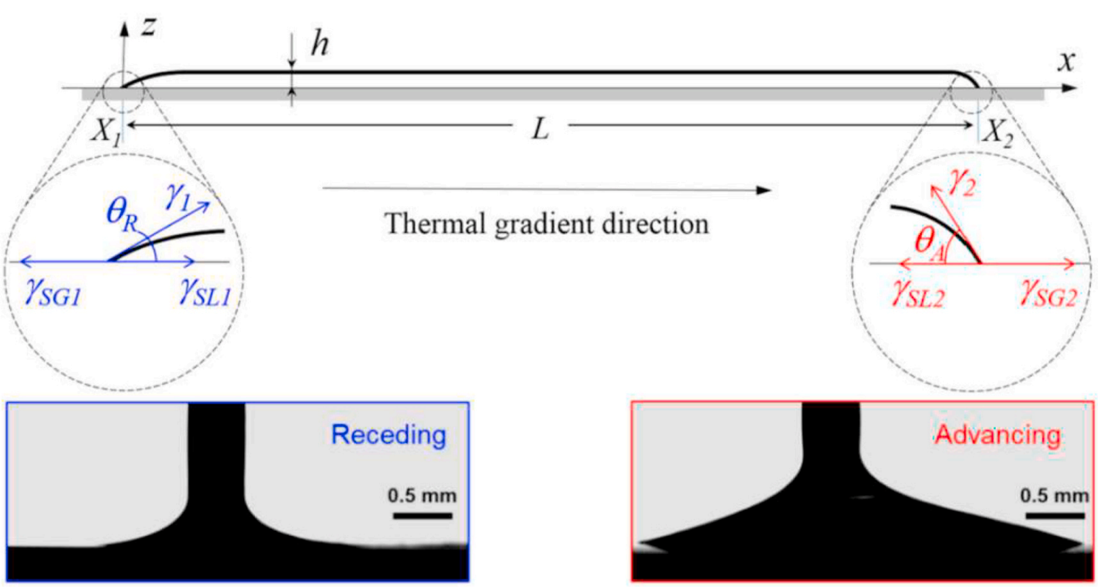

Fig. 10. Droplet migration model on an ideal surface with the advancing and receding contact angles shown at the rims [85].

3.1.4. Gravity effect

The profile of liquid droplets resting on a horizontal surface depends on the contact angle at the triple-phase interface. When the surface is tilted, the contact angle and the shape of droplets change due to the gravity, especially for the partial wetting droplets [114–116]. By taking the gravity effect into consideration, the migration on an incline can be obtained as [105]:

$$U = \frac{1}{g(x_A, x_R)} \frac{(1 + 2\cos\theta)\gamma_T C_T L \pm 2Mg\sin\phi}{6\mu_0} h \tag{10}$$

where ϕ is the inclination angle. The operator of plus or minus depends on the inclination direction. Positive inclination means that the droplet would migrate from top to bottom, which would contribute to the migration. The predictions of the migration velocity on surfaces with various inclination angles are shown in Fig. 11.

3.1.5. Types of thermal gradient

For the unidirectional thermal gradient, it is understandable that droplets tend to migrate from the high temperature (left) to low temperature (right) regions. However, when the thermal gradient is omnidirectional, the droplets tend to migrate radially outward from the center to the surrounding region, forming a ring-like motion, as shown in Fig. 4b [29]. This is a totally different interfacial phenomenon, in which the thermal gradient induced unbalanced interfacial tension can be bifurcated into the radial and peripheral directions. The radial one provides the necessary propulsion for the migration to the surroundings while the peripheral one acts on the adjoining liquid and contributes to the ring-like shape. Dai et al. proposed an experimentally-verified model for estimating the velocity of the ring-like migration as follows:

$$U = \frac{\gamma_T C_T h}{12\mu_T}\left[4\cos\theta \frac{R_A - R_R}{R_A + R_R} + 1\right] \tag{11}$$

where $\mu_T = \mu_0 e^{b\left[C_T\left(\frac{R_A+R_B}{2}\right) - T_{Start} + T_0\right]}$.

While analytical expressions readily provide a clear relationship between the different parameters involved and enable one to gain physical insight into the problem, treatment of complex geometrical configurations and multiplicity of intertwined factors involve often require one to resort to numerical solutions, particularly when prediction accuracy is of primary concern. Progress toward available numerical treatment approaches is reviewed in Section 3.2.

3.2. Numerical simulation

3.2.1. Numerical approaches

Computational fluid dynamics (CFD) is an indispensable tool for investigating the flow characteristics. In the field of thermocapillary migration, CFD has been successfully employed to understand, explain, and reveal its complex flow mechanisms [89,117–126]. Many numerical approaches, including level set, the volume of fluid, moving mesh, front tracking, Lattice Boltzmann, and molecular dynamics, have been successfully employed to simulate the migration on free solid surfaces. Table 2 shows a summary and comparison of the reported numerical approaches for simulating the thermocapillary migration and provides remarks on the advantages and limitations of each numerical approach.

3.2.2. Guidelines for numerical simulation

Referring to Table 2, the following general recommendations are made (see Fig. 12).

Controllable conditions and properties [127–132,147–150]. For numerical approaches, the property of liquids and solids, including the contact angle, viscosity, surface tension of liquids, materials, surface morphology, wetting property (slip condition) of solids, can be assigned in a wide range. Besides, extreme conditions of a thermal gradient, pressure, and gravity-free can be treated by numerical simulations of the governing equations with variable properties. Numerical approaches provide controllable conditions and properties that cannot be easily achievable in experimental methods. See, for example, the migration

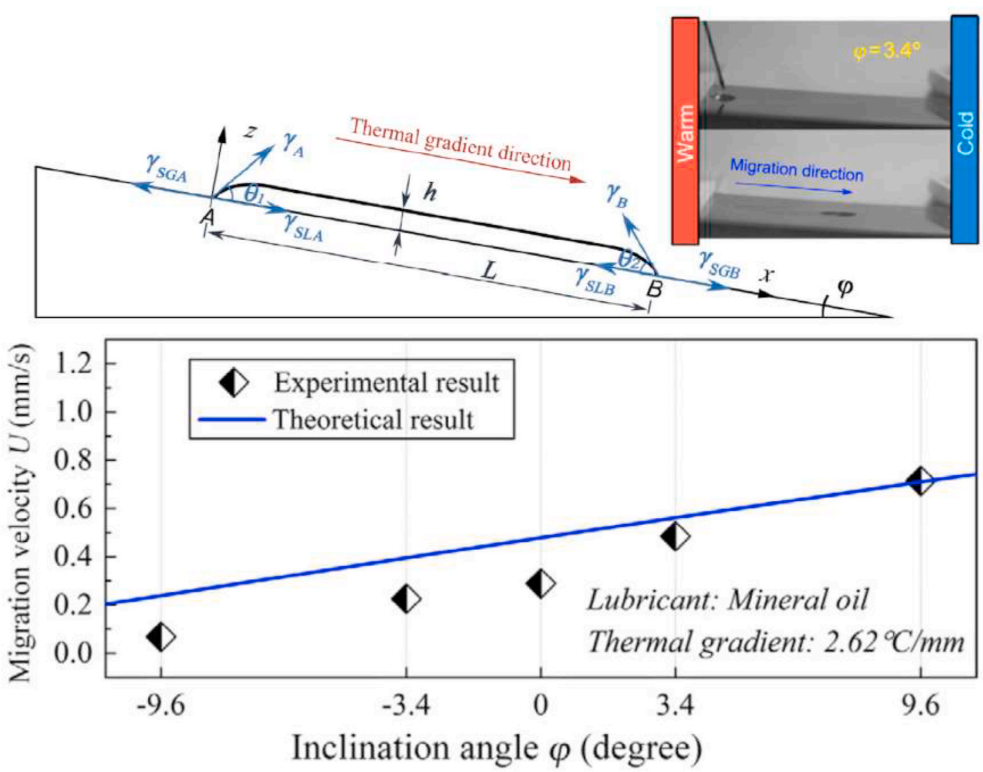

Fig. 11. Thermocapillary migration of mineral oil droplets on inclined surfaces [105].

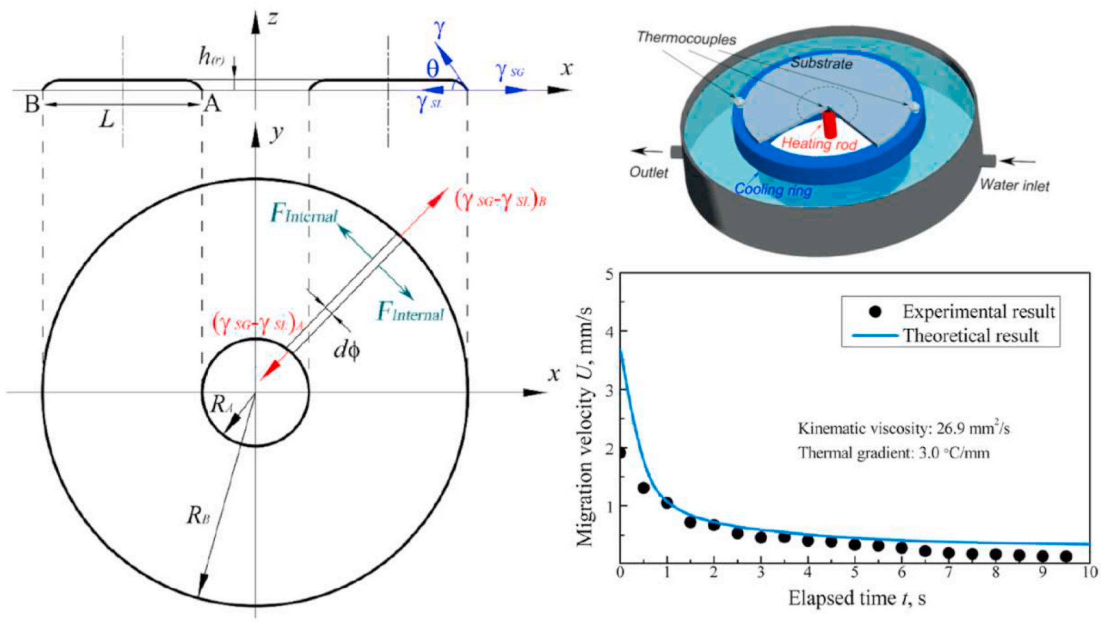

Fig. 12. Thermocapillary migration of paraffin oil droplets on the smooth surface induced by an omnidirectional thermal gradient [29].

Table 2
Summary and comparison of the reported numerical approaches for simulating the thermocapillary migration.

Approaches	Applications	Limitations	References
Level set	≻Suitable for small scale-free liquid surface. ≻Fluid is sensitive to its surface tension. ≻Fluid properties pass smoothly from liquid to gas. ≻High accuracy.	✧Need to reinitialize the function. ✧Slow simulating speed. ✧Computationally expensive for complex or 3-D models.	Borhana et al. [127]; Raessi et al. [128]; Yi et al. [129]; Chen et al. [130,131]; Ding et al. [132].
Volume of fluid (VOF)	≻Well-developed for immiscible fluids. ≻Easy to couple with CFD solver. ≻High efficiency. ≻Low space.	✧Limited accuracy for fluid dynamics.	Chieng et al. [133]; Alhendal et al. [134,135]; Mostaghimi et al. [136]; Chakraborty et al. [137]; Bothe et al. [138,139].
Moving mesh	≻Simply and straightforward. ≻Defined girding points. ≻Surface forces are applied as boundary condition.	✧Ignore gas effect for accelerating simulation. ✧Unable to handle the topological version in free fluids.	Yin et al. [140]; Liu et al. [141]; Chen et al. [142]; Lu et al. [143].
Front tracking	≻Similar to VOF.	✧Fails on complicated interface.	Nas et al. [144]; Yin et al. [145]; Wu et al. [146].
Lattice Boltzmann method (LBM)	≻Volume-less particles. ≻Scale between Navier-stokes (N–S) and MD.	✧Under development. ✧To be validated.	Liu et al. [147–150].
Molecular dynamics (MD)	≻Well-developed in biophysics. ≻Molecular scale.	✧Computationally expensive. ✧Unable to verify via experiments. ✧To be validated in migration.	Li et al. [151]; Maroo et al. [152]; Chakraborty et al. [153]; Foroutan et al. [154]; Wang et al. [155].

results are shown in Fig. 13a (contact angle of 70°), Fig. 13b (contact angle of 120°) and Fig. 13c (contact angle of 90°) are calculated via numerical approaches of level set, Lattice Boltzmann method, and volume of fluid.

Detailed migration-related physical fields [132–143]. The evolution of temperature distribution on the solid surface, the exchange of heat among the solid-liquid-gas phases as well as the fluid-thermal-solid interactions can be easily simulated numerically. The thermal gradient induced forces acting on the liquid can be identified and interpreted, and the corresponding migration processes, especially the inner flow fields, can be illustrated. Moreover, with appropriate governing and boundary equations, the dynamic receding/advancing contact angles across the liquids can be predicted. These migration-related physical fields provide enough information for understanding and explaining the mechanism, which are very good additions to experiments.

3D visualization [139]. The 3D model is one of the optimal choices to model the real physical processes, especially when varying conditions need to be taken into consideration. Physically, extending 2D to 3D is not too difficult, and evaluating of a 3D model could achieve more accurate predictions and information on the migration at the expense of a large amount of computational time and additional complications in the derivations and treatment. The 3D simulation by Bothe et al. [139] (Fig. 13c) has proven its advantage. Nevertheless, the current difficulties are how to control the convergence and resolution under an acceptable computation time. It is expectable that with the advances of computer technology and numerical methodologies, 3D visualization can be realized in the future.

Insights at molecular level [151–154]. Molecular dynamics (MD) simulations are widely used to explore the microscopic interactions at the molecular level. As the work by Foroutan et al. [154] in Fig. 13d

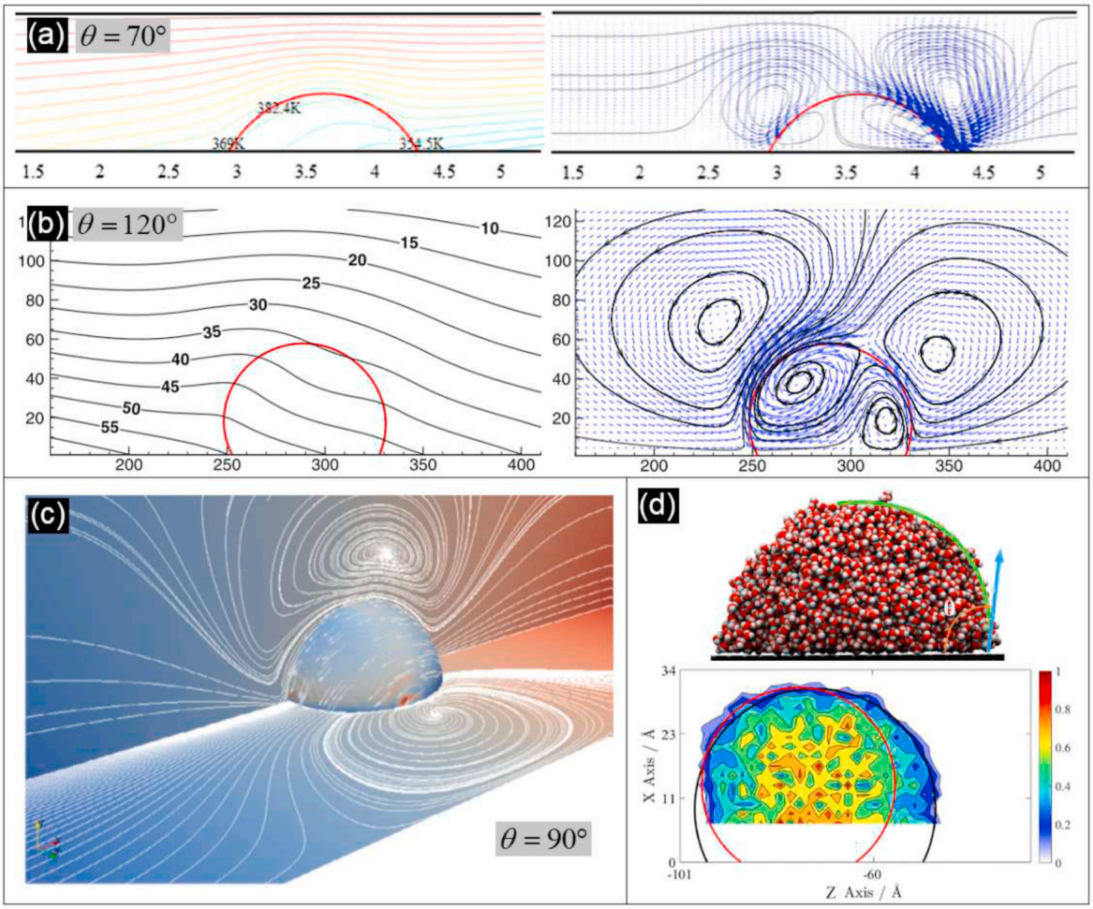

Fig. 13. 2-D temperature field (the left plane) and flow field (the right plane) of the moving droplets on (a) a hydrophilic surface with a contact angle of 70° [142] and (b) a hydrophobic surface with a contact angle of 120° [147]. (c) 3-D temperature and flow fields of the moving droplet under a thermal gradient of 10 °C/mm and contact angle of 90° [139]. (d) Graphical representation of the droplet contact angle and mass-density contour plot of the nano-droplet at t = 0.7 ns and 393 K [154].

indicates, MD simulation provides the translational and vertical motions of liquid molecules subjected to a thermal gradient. They considered the contact angle hysteresis effect, and the numerical trend is consistent to experimental ones. In comparison to other methods, the unique feature of MD simulation is the insights into the molecular level, which could provide some feasible anti-migration design strategies for new lubricants or lubricant additives.

Note that the above-mentioned recommendations or guidelines can be adapted for different purposes and applications. Thermocapillary migration is a highly complex process, which involves the coupling of thermal equilibrium, kinetics, heat and mass transfer, and computational fluid dynamics. This complexity has currently prevented the proposed theoretical/computational models in the literature from achieving the required accuracy for optimizing the migration process. Based on the numerical purpose and application, accurate results can be achieved by careful selections of the type of numerical solution scheme, mesh, convergence criteria, methods for specifying boundary conditions, etc.

4. Manipulation strategies

Understanding the mechanism of thermocapillary migration is the most important precondition, which is quite instructive for the design of manipulation strategies. In the following sections, we summarize the available strategies over the past decades.

4.1. Liquid aspect

As mentioned in Section 2.3, a liquid with a higher viscosity has a lower migration velocity due to the significant viscous resistance force. It is well-known that additives are essential parts of the modern lubricants for accomplishing a variety of functions such as control friction and reduce wear [156–158]. The usage of appropriate additives is an effective approach to regulate the movement [159–165].

Yang et al. [166] found that the thermocapillary migration of droplets is significantly depressed by the introduced water-soluble surfactants. In fact, they showed that Sodium dodecyl sulfate and Triton X-100 could completely inhibit the thermocapillary effect. Chakraborty et al. [167] theoretically investigated the motion of a surfactant-laden viscous droplet in the presence of non-isothermal Poiseuille flow and found that the surfactant induced Marangoni stress affects the droplet velocity, which depends on the direction of the temperature gradient with respect to the imposed Poiseuille flow. Wang et al. [168] experimentally studied the effect of typical lubricant additives of anti-wear (Zinc dialkyldithiophosphates, ZDDP), ashless dispersant (polymer succinimide), anti-foam (polydimethylsiloxane), and oiliness (oleic acid) on the thermocapillary migration and surface tension coefficient, as shown in Fig. 14. Their results revealed that using additives to enhance the adsorption of liquids on solid surfaces (oleic acid) [169] or by decreasing the surface tension coefficient of liquids (polydimethylsiloxane) can slow down the migration effectively. For additives that can increase the surface tension coefficient of liquids, reducing their contents in liquids is suggested to weaken the migration.

4.2. Solid aspect

As mentioned in Section 2.3, the thermocapillary migration phenomena of liquids on different solid surfaces are different. Generally, a smooth surface of higher surface free energy can strongly grasp a liquid, exhibiting a more significant anti-migration capacity. Given that engineering surfaces are rough and contain micro flaws and defects, these surface features can pin the contact line of a droplet on surfaces. Researchers are inspired to manipulate the migration via surface structures. Many different types of surface treatments including roughening the solid surfaces, fabricating isotropic, anisotropic, or hierarchical structures patterns, overlaying wettability coatings have proven to be feasible manners to regulate the migration. For the guidance of the design of tribological components encountered with thermal gradients, these strategies are classified and discussed as follows.

4.2.1. Surfaces roughness

In 1979, Fote et al. [170] found that roughening solid surfaces with sharp edges (~2 mm) or fabricating scratch around edges were effective in preventing lubricants migration (Fig. 15a). Although these macroscopically rough structures are not always practical for implementation on rubbing surfaces, it cast an early vision on preventing the migration through surface structures. Klien et al. [171] investigated that the migration behavior on a ground surface with scratches in the direction of the thermal gradient and found that surface scratches can converge the lubricant as the migration progresses (Fig. 15b). Wang et al. [39] confirmed that a surface with grinding scars angular to the thermal gradient could obstruct the migration to some extent (Fig. 15c). Bai et al. [172] found that on rough surfaces, a directional lubricant migration would occur when the temperature gradient was large enough; otherwise, lubricants tended to move in both directions (Fig. 15d). Dai et al. [173] further proved that decreasing the surface roughness (Sa) or the surface developed interfacial area ratio (Sdr) can enhance the obstruction effect (Fig. 15e).

4.2.2. Regular patterned microstructures

Given that surface roughness is "random" in nature, its effect on the thermocapillary migration cannot be controlled accurately. Hence, regular patterned microstructures can be designed on the surfaces to achieve controllable effects on the thermal flow. Zhou et al. [174] fabricated a regular pattern of oleophobic microdimples on titanium surfaces, which can firmly confirm lubricants at the designed area (Fig. 16a). Dai et al. [175] found that even without oleophobicity property, the pattern of microdimples can impede thermal capillary migration under omnidirectional thermal gradients effectively (Fig. 16b). Except for microdimples, microgroove is another representative structure. Wang et al. [176] revealed that aligned microgrooves could restrict the lubricant migration easily in the direction perpendicular to the thermal gradient while guiding the migration in the parallel direction (Fig. 16c). This acceleration effect of microgrooves in the parallel direction was also confirmed by other researchers [88, 177–179]. Grutzmacher et al. [180,181] found that multi-scale microgrooves patterns can yield a faster migration rate than the single-scale ones (Fig. 16d).

The acceleration and deceleration properties of the above-mentioned regular patterned microstructures are very attractive. Gradients are omnipresent in nature, and researchers have successfully fabricated geometry, density, and arrangement of microgrooves pattern with gradient configurations to achieve better regulation performances.

4.2.3. Topographical gradient microstructures

Geometry and density are two typical gradient configurations in designing microgrooves pattern. Kooij et al. [182] prepared stripe-patterned gradient surfaces by changing the width of microgrooves on which liquid droplets can move spontaneously (Fig. 17a). Similarly, fabricating gradient surfaces with increasing density of microgrooves pattern (Yang et al. [183], Fig. 17b) or decreasing density (Lai et al. [184], Fig. 17c) can all activate locomotion of liquid droplets. Except for the density of microstructures, the gradient of the geometric dimension of the microstructure itself is also feasible for the controllable ability. Hao et al. [185] designed a scale-gradient micropillars pattern on hydrophobic surfaces to drive the movement of liquid droplets (Fig. 17d), and the density gradient also works for micropillars [186]. Combining density and scale gradient together, Sommers et al. [187] designed a topography-based gradient microgroove patterned surface, which can control the movement of liquid droplets in the direction perpendicular to the grooves (Fig. 17e).

4.2.4. Radial gradient microgrooves

Expect the above aligned configuration, microgrooves pattern can be designed with a radially gradient. As shown in Fig. 18a, Franssila et al. [188] prepared a radial groove pattern with continuous topography gradient, which induces a continuous inward wettability gradient and enables self-propelling. Similarity, Davis et al. [189] fabricated a hydrophobic micropatterned surface with grooves size increases outward gradually; this surface can continuously transport liquid droplets along these structures (Fig. 18b). Bliznyuk et al. [190] also designed a radial groove pattern with decreasing width hydrophobic property on a hydrophilic substrate, which can guide the liquid motion spontaneously (Fig. 18c). Dai et al. [87] studied the thermocapillary migration on radially microgrooved surfaces and confirmed that migration could be enhanced on the convergent direction, and increasing the initial

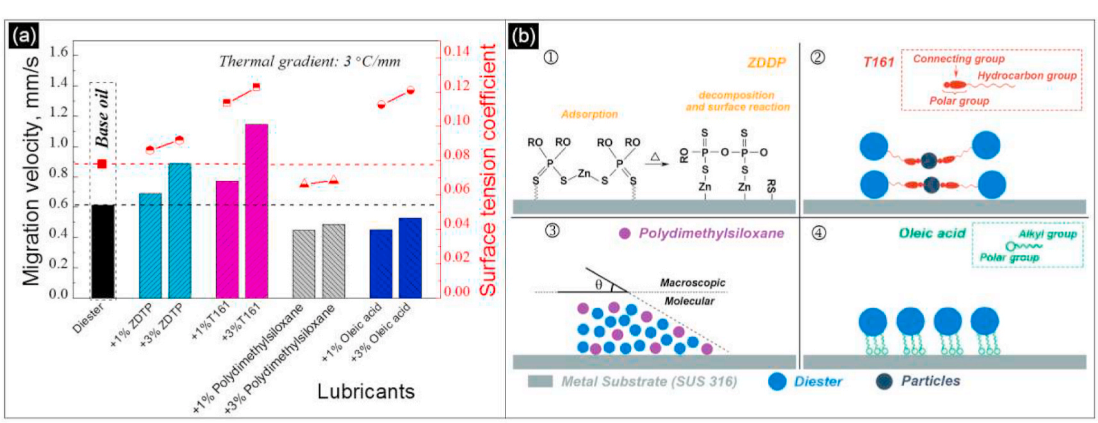

Fig. 14. (a) Influences of typical lubricant additives of ZDDP, T161, polydimethylsiloxane, and oleic acid on the migration behavior and surface tension coefficients in the base oil of diester. Mechanism of (b) anti-wear film formation of ZDDP on the metal surface, (b②) interactions among dispersant/particles/diester, (b③) interactions between polydimethylsiloxane and diester, (b④) interactions among oleic acid/diester/metal surface [168].

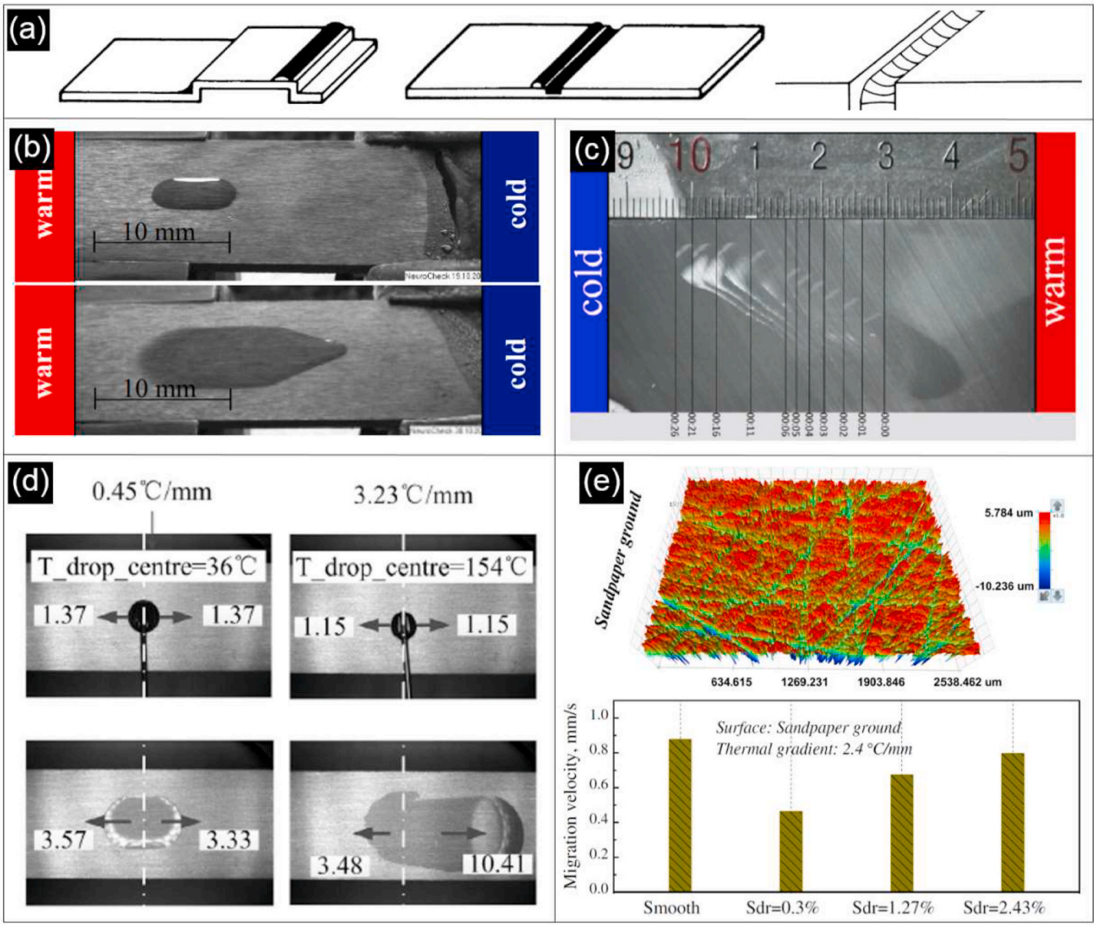

Fig. 15. (a) Anti-migration structures on surfaces with sharp edges and scratch around the edge [170]. (b) Migration on a ground surface with scratches in the direction of the thermal gradient [171]. (c) Migration on a surface with grinding scars of 60° angular to the thermal gradient [39]. (d) Migration in both directions on a rough surface under a thermal gradient of 0.45 °C/mm, while in a unique direction under a thermal gradient of 3.23 °C/mm [172]. (e) Effects of surface roughness on the migration behavior [173].

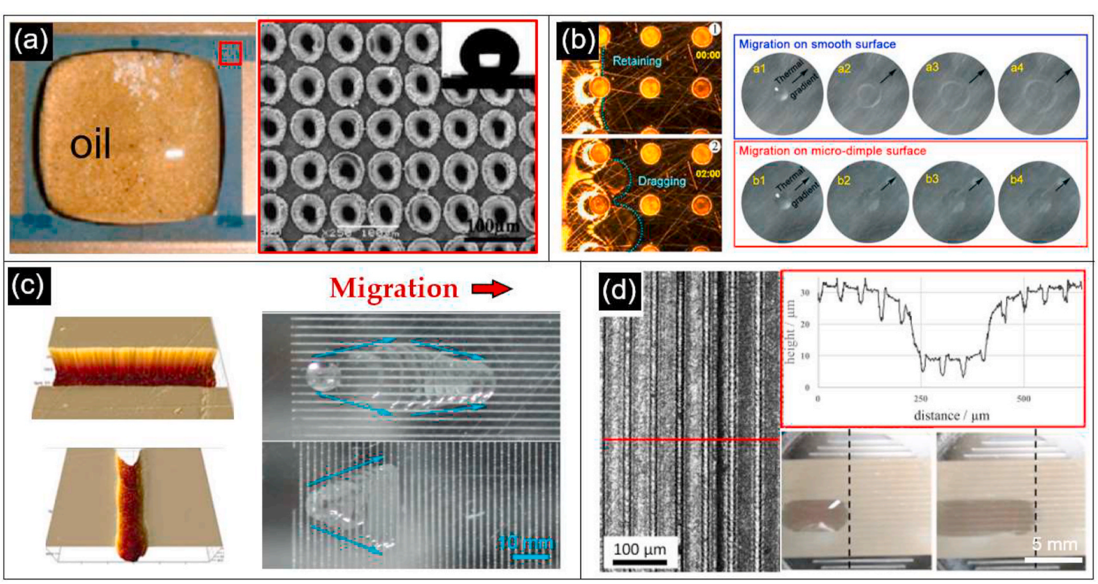

Fig. 16. (a) Anti-migration surface featured with superoleophobic microdimples pattern [174]. (b) Obstruction effect of a single dimple when a lubricant migrates to it [175]. Migration phenomena on surfaces with (c) microgrooves patterns parallel and perpendicular to the thermal gradient [176], and (d) multi-scale and single-scale microgrooves patterns [180].

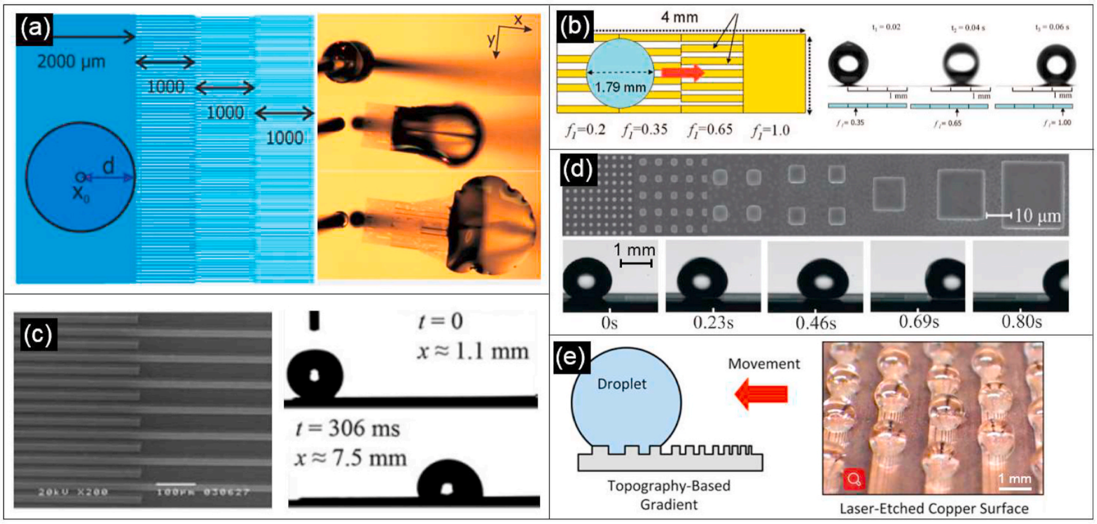

Fig. 17. (a) A width-gradient pattern configuration and spontaneous movement of a liquid droplet on the designed surface [182]. Profiles of density gradient patterned surfaces and droplets transporting process: (b) increasing density [183] and (c) decreasing density [184]. (d) Scale-gradient micropillars pattern to drive the locomotion of liquid droplets [185]. (e) Sketch of the topography-based gradient microgroove patterned surface and self-driving movement of a liquid droplet on it [187].

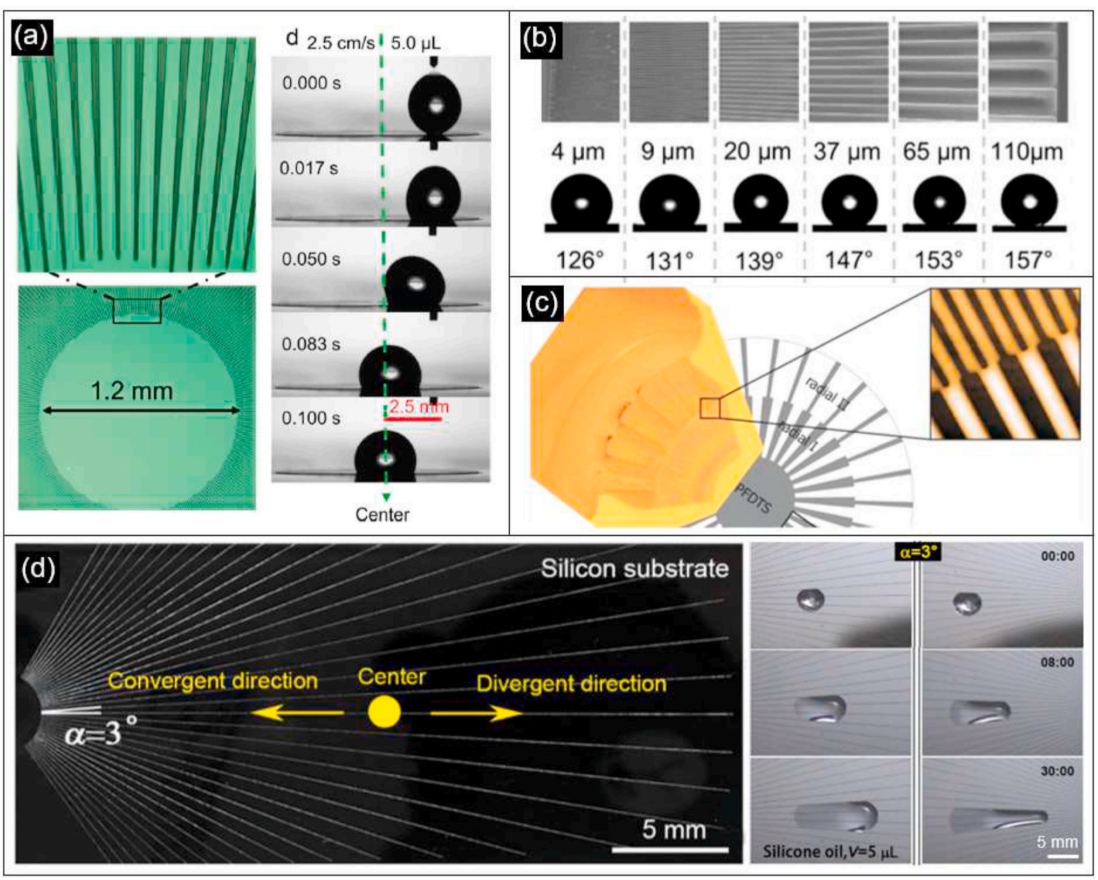

Fig. 18. (a) Radial groove pattern of continuous topography gradient and the self-propelling movement of droplets on it [188]. (b) Micropatterns with groove size increases outward, on which the wettability increases correspondingly [189]. (c) Radial groove pattern with a decreasing width of hydrophobic property on a hydrophilic substrate [190]. (d) Thermocapillary migration on radially microgrooved surfaces in convergent and divergent directions [87].

divergence would weaken its contribution (Fig. 18d).

4.2.5. Wedged microgrooves

The microstructure itself can have a gradient feature, and the wedged groove is a very typical one [191–193]. Nakashima et al. [194] prepared a hydrophilic film with wedged microgrooves on a hydrophobic substrate to drive the movement of liquid droplets (Fig. 19a). This type of wedged pattern is also feasible at the millimeter scale, Eid et al. [195] fabricated a wedge-shaped hydrophilic aluminum on a hydrophobic copper surface for propelling liquid droplets (Fig. 19b). When a surface is fabricated with a connected pattern of wedged microgrooves, it can drive mobile Leidenfrost droplets [196] (Fig. 19c). Dai et al. [197] reported that the driving capacity of wedged microgrooves strongly depends on the shape of the connecting corner and that smooth corners have a better acceleration effect than the sharp ones (Fig. 19d). When the wedge-shaped microgrooves are unconnected and concave at the bottom, it can also guide the liquid movement effective [25] (Fig. 19e). Moreover, properly designing the geometric parameters of wedged grooves including the angle of divergence (Fig. 19f) [198], multi-shape (Fig. 19g) [199], multi-scale (Fig. 19h) [200], or tree-shaped hierarchical pattern (Fig. 19i) [201], can either strengthen or weaken the liquid motion, which depends on the aforementioned topographical characteristics.

Overall, by taking advantage of topographical complexities, researchers have made significant progress in direct and spontaneous transport of liquids on solids, and the above-mentioned strategies are just parts from the published literature. Attributing to the rapid development of precision machining technologies, a huge number of milli-, meso-, micro-, and nano-scaled structures of topographical complexities [202–214], have been designed and fabricated to manipulate liquid motion, we are not going to discuss them in details due to the limited space.

4.3. Chemical gradient coatings

It should be mentioned that fabricating physical structures on solid surfaces could inevitably damage the surfaces, which brings in some undesired defects in actual applications. To this end, chemical coatings have certain advantages. Roberts et al. [215] found that painting low surface energy materials, such as fluorocarbon compounds around rubbing areas, can create a barrier to confine lubricant migration in the space components. As the forces balance at the vicinity of the three-phase contact line shown in Fig. 5, a low surface energy coating diminishes the solid/gas interfacial tension (γ_{SG}), and this decrease can impede the spreading capacity of a liquid on a solid. According to Eq. (2), if the low surface energy coatings are not uniformly distributed on solids, the solid/gas interfacial tension differences can yield various external force acting on liquids. The pioneering work of Chaudhury et al. [216] proved that a surface with a spatial gradient in its surface free energy was capable of causing drops of water placed on it to move uphill, and he successfully fabricated gradient surfaces by allowing the vapor of decyltrichlorosilane to diffuse over a silicon wafer.

Inspired by this finding, researchers have made great progress in designing and fabricating gradient surfaces. Surface-chemical gradients are surfaces with chemical properties that gradually change within a given distance [217,218]. The chemical gradients can be created according to two basic principles: either the outermost surface layer of a substrate is gradually modified, or a surface coating is attached to the surface in a gradual manner. Technically, the gradient surfaces are commonly fabricated via two main systems: self-assembled monolayers (SAMs) and polymer coatings [219–221]. Here, these two system-based fabrication techniques are summarized for guiding the regulation strategies on thermocapillary migration.

SAM-based technique

Dip-coating is one of the most simple and reproducible approaches to fabricate surface-chemical gradients [222]. By means of a gradual immersion, adsorption of molecules from dilute solutions (Fig. 20a [223]), or equivalently, desorption of molecules into dilute solutions (Fig. 20b [224]), can be accurately controlled to fabricate gradient coatings. Besides, cyclic draining-replenishing the solutions (Fig. 20c [225]), draining or injecting the solutions gradually [226,227], can also achieve the gradient coatings. The key point in fabricating gradient surfaces is to control the chemical reaction time or the duration time between chemical medium and solids. Fig. 20d presents images of water droplets on a solid surface achieved via the SAM-based technique [228], of which the wettability decreases gradually in the horizontal direction. Note that via choosing appropriate parameter combinations of solvent, the concentration of the solution, immersion time, velocity, acceleration and temperature, one can even construct a coverage gradient of one molecule, and complex coatings, such as multi or hierarchical coatings, can be achieved by saturating with another component during a subsequent immersion. Besides the above-mentioned techniques, ASM-based surfaces with a chemical gradient can also be achieved via

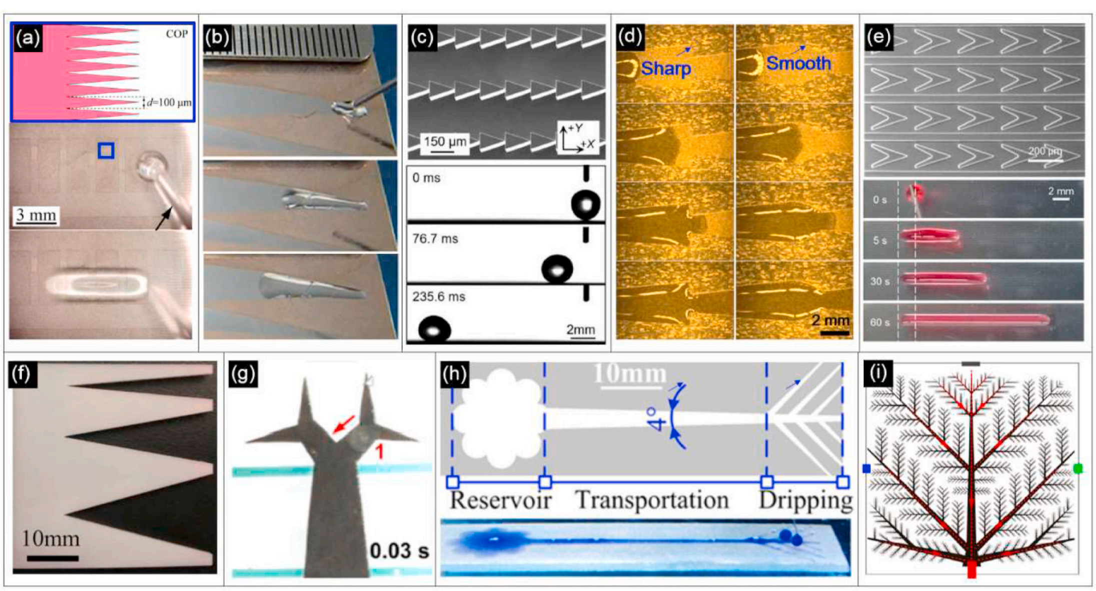

Fig. 19. A surface with wedge-shaped patterns for wettability gradient at (a) microscale [194] and (b) millimeter scale [195] and the automatic droplet transportation process. (c) A surface with connected wedged microgrooves pattern and the rectified mobile Leidenfrost droplets [196]. (d) Movements of paraffin oil droplets on surfaces with patterns of wedged microgrooves of sharp and smooth corners [197]. (e) A surface with unconnected wedge-shaped microgrooves and concave at the bottom, and the directional transport of paraffin oil [25]. Derived topography of wedged grooves of (f) increasing angle of divergence [198], (g) multi-shape [199], (h) multi-scale [200], (i) tree-shaped hierarchical pattern [201].

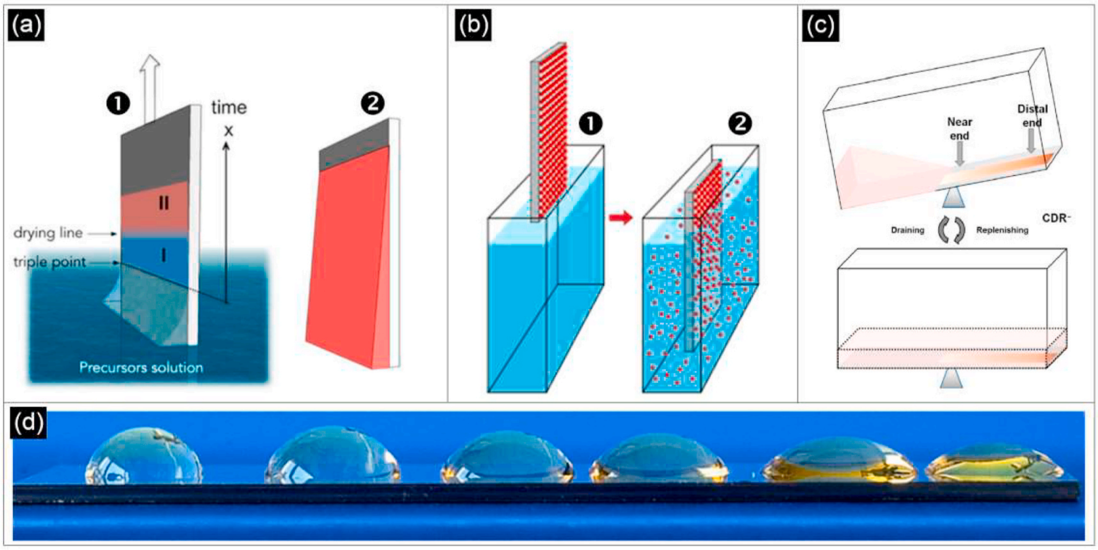

Fig. 20. (a) Dipping and coating deposition [223], (b) dipping and degrafting the pre-attached molecules layer [224], and (c) cyclic draining-replenishing the solutions [225] processes for the formation of gradient surfaces. (d) Water droplets on a surface with a wettability gradient [228].

evaporation-adsorption [219], chemical vapor deposition (CVD) [229], gradual oxidation by UV irradiation [230] or laser [231], and thermal treatment [232,233].

Polymer-based technique

The most common way to fabricate gradient polymer architectures is by means of a polymer brush, in which polymer chains are terminally tethered to a surface. The preparation of a polymer brush can be divided into two categories of grafting onto and grafting from the surfaces. The first one is a "top-down" graft method that polymer chains are directly bonded to the surface. The second one is a "bottom up" method that molecular brushes are growing on the surface via grafting from the or surface-initiated polymerization. Via these approaches, it is feasible to create monolayers of a variety of polymers with a thickness between a few nanometers and micrometers, and the properties of the layers can be readily adjusted by choosing an appropriate monomer [234–238].

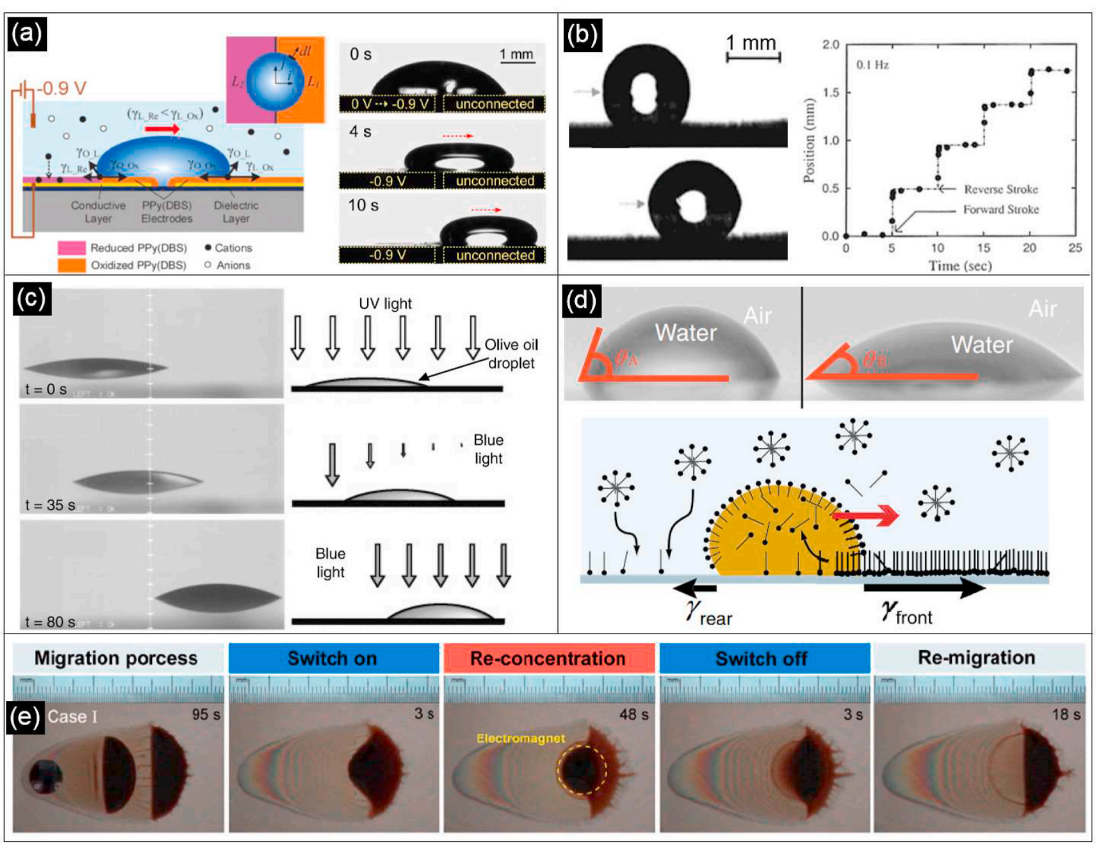

Fig. 21. Regulating liquid via external fields of (a) electrical [246], (b) mechanical oscillatory [261], (c) photoirradiation [250], (d) nonequilibrium noise [253], (e) magnetic [257].

4.4. External fields

In addition to the above-mentioned strategies at liquid and solid aspects, introducing complex external fields of electrical [239–247], oscillatory [96,97,248,249], photoirradiation [250–252], acoustic wave [253,254], magnetic [255–260] are also feasible manners to regulate droplets motion, and some typical findings are exhibited in Fig. 21. Yang et al. [246] designed conjugated polymer electrodes to actuate the motion of organic droplets (Fig. 21a). Chaudhury et al. [261] successfully realized the motion of liquid drops on solid surfaces by vibration (Fig. 21b). Ichimura et al. [250] reversibly manipulated the macroscopic motion of liquids by photoirradiation (Fig. 21c). Via non-equilibrium noise, Magome et al. [253] constructed a regular motion of liquid (Fig. 21d). Wang et al. [257] proposed a magnetic switch using an electromagnet to control the migration and re-concentrate the migrated lubricants (Fig. 21e).

Essentially, these manipulation methods are all based on the surface tension gradient frame. That is, a proper design of external fields can change the surface tension of liquid, disequilibrating the interfacial tensions at the surface/interface, yielding a locomotion. It should be noted that although these methods are accurate, efficient and effective, obvious drawbacks exist that are complex, expensive, and with additional manipulation, which is difficult for practical applications.

5. Outlook

Overall, the current investigations on the thermocapillary migration of liquids, from the fundamentals to the evaluations, and the corresponding manipulation strategies, is systematically summarized, and these gradual researches provide deepening insights into the interfacial phenomenon. With the development of experimental technologies and theoretical innovations, many unsolved mysteries on this thermocapillary migration could have significant progress in the further. We would like to share our opinions on the thermocapillary-related research contents and the potential difficulty.

5.1. Thermocapillary migration of liquid lubricants at different interfaces

Up to now, most of the reported researches on the thermocapillary migration are on free surfaces. Drawing attention back to practical applications, one should note that there are many situations where liquids exist at different interfaces. For example, thermocapillary migration occurring in tribo-components of rolling or sliding bearings is indeed at the interfaces between sphere/plate or plate/plate. Although researchers have known the fact that migration would occur at typical friction pairs with relative speed, the current level of physical understanding is mostly obtained from the observed side effects. For example, in rolling bearings, when the friction coefficient rises rapidly under extreme temperatures, it is inferred that thermocapillary migration of liquid lubricants must have occurred. Direct observations on the thermocapillary migration at different interfaces with a relative motion are currently lacking.

Recently, the authors reported an investigation of the Thermocapillary migration of lubricants at different stationary interfaces [262,263]. As shown in Fig. 22, it is found that liquid lubricants can easily migrate at the free surface and the plate/plate interface while maintains at the sphere/plate interface for a long time, accompanied by a continuous loss of a thin liquid film at the cold side. It means that thermocapillary migration at varying interfaces is entirely different. However, this work represents a preliminary experimental exploration of the thermocapillary migration at stationary interfaces. The physical mechanism of thermocapillary migration at interfaces with a relative motion is still not clear. The important and difficult points are how to construct an experimental apparatus contains two rubbing surfaces with controllable relative speeds and thermal gradients. Castrejon et al. [264] designed an apparatus to observe the droplets onto moving liquid surfaces, which provides a feasible method to analyze the motion of liquid on other moving surfaces. Combining this experimental principle with typical tribological machines of pin-on-disk [265] or face-to-face [266], or common mechanical seal tester [267], investigations on the migration at moving interfaces can be investigated. Besides, the corresponding mechanism can be realized via both numerical modeling and theoretical

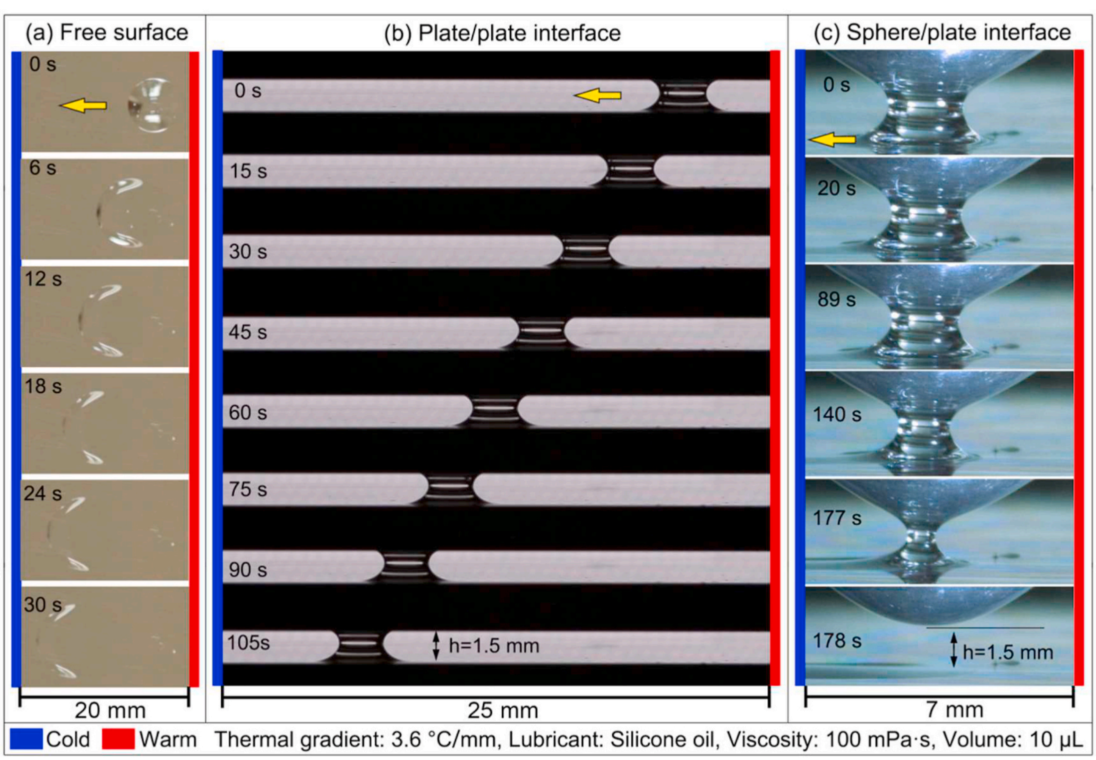

Fig. 22. Thermocapillary migration of liquid lubricants at different interfaces of (a) plate/air (free surface), (b) plate/plate, and (c) sphere/plate [262].

derivation.

5.2. Regulating thermocapillary migration at different interfaces

With the understanding of the mechanism of thermocapillary migration at moving interfaces, the regulation and control strategies are worthy of further study. Compared to the vast reported regulation strategies on free solid surfaces, research on manipulating thermocapillary migration at different interfaces is just getting started. It is expectable that continuous relevant researches on regulating the thermal flow at different interfaces from the aspects of solids, liquids, and external fields, would be a meaningful research hotspot and attract a lot of attentions.

5.3. Migration at micro or nano scales

Except for the already known thermocapillary migration of liquids at milli- or meso-scales, migration at micro or nanoscale deserves further investigation. In the experimental aspect, for instances, thin liquid lubricant films with a monolayer or a few layers of perfluoropolyether are often chosen for lubrication in magnetic recording disks, and their thickness is as small as 0.1 Å [18]; In elastohydrodynamic lubricated (EHL) contacts, starvation often occurs due to limited lubricant replenishment at high speeds [23]. Moreover, for molecular thin liquid films, disjoining pressure involves the spreading and dewetting of liquid droplets. Thus, understanding the underlying driven forces is of significant importance to properly assess the behavior of droplets on solid surfaces [268,269]. On the basis of the existing techniques such as optical surface analyzer or optical interferometry film tester and by integrating the temperature control system on them, micro or nanoscale migration can be realized. In the theoretical aspect, trans-scale modeling or simulation is still an unsolved problem. Establishing a relationship between experiment and theoretical results is of great significant important for optimizing theoretical models and corresponding boundary conditions. Further investigation of these aspects could produce fruitful findings.

In summary, research on the thermocapillary migration of liquids at different interfaces is still in its infancy. The inherent science issues, including the basic mechanism, the theoretical/numerical models, and the manipulation strategies are currently unsolved. Investigation on these aspects has significant theoretical guidance and practical application value. Future findings are expected to serve in high-performance mechanical components in aerospace or deep space exploration, such as boundary lubrication bearings in the helicopter transmission system, the sealing interfaces of the principal bearing cavity of aircraft engine, liquid bearings in space, and the like.

Declaration of competing interest

The authors declare that they have no known competing financial interests or personal relationships that could have appeared to influence the work reported in this paper.

Acknowledgments

The authors from Nanjing University of Aeronautics and Astronautics are grateful for the support provided by the National Natural Science Foundation of China (grant No. 51805252).

References

[1] Marangoni C. Sull'espansione delle gocce di un liquido gallegianti sulla superficie di altro liquido (on the expansion of a drop of liquid floating on the surface of another liquid). Tipografia Dei Fratelli Fusi; 1865.
[2] Levich VG, Krylov VS. Surface-tension-driven phenomena. Annu Rev Fluid Mech 1969;1:293–316.
[3] Nikolov A, Wasan D, Lee J. Tears of wine: the dance of the droplets. Adv Colloid Interface Sci 2018;256:94–100.
[4] https://www.Comsol.Com/blogs/tears-of-wine-and-the-marangoni-effect/.
[5] Cazabat AM, Heslot F, Troian SM, Carles P. Fingering instability of thin spreading films driven by temperature gradients. Nature 1990;346:824–6.
[6] Velarde MG, Zeytounian RK. Interfacial phenomena and the marangoni effect. Springer; 2002.
[7] Bormashenko E, Bormashenko Y, Grynyov R, Aharoni H, Whyman G, Binks BP. Self-propulsion of liquid marbles: leidenfrost-like levitation driven by marangoni flow. J Phys Chem C 2015;119:9910–5.
[8] Scriven LE, Sternling CV. The marangoni effects. Nature 1960;187:186–8.
[9] Xu XF, Luo JB. Marangoni flow in an evaporating water droplet. Appl Phys Lett 2007;91:124102.
[10] Tadmor R. Marangoni flow revisited. J Colloid Interface Sci 2009;332:451–4.
[11] Pearson JRA. On convection cells induced by surface tension. J Fluid Mech 1958;4:489–500.
[12] Young NO, Goldstein JS, Block MJ. The motion of bubbles in a vertical temperature gradient. J Fluid Mech 1959;6:350–6.
[13] Dai QW, Khonsari MM, Shen C, Huang W, Wang XL. Thermocapillary migration of liquid droplets induced by a unidirectional thermal gradient. Langmuir 2016;32:7485–92.
[14] Kubotera H, Bogy DB. Effect of various physical factors on thin lubricant film migration on the flying head slider at the head-disk interface of hard disk drives. J Appl Phys 2007;102:054309.
[15] Singer JP. Thermocapillary approaches to the deliberate patterning of polymers. J Polym Sci B Polym Phys 2017;55:1649–68.
[16] Chakraborty M, Ghosh UU, Chakraborty S, DasGupta S. Thermally enhanced self-propelled droplet motion on gradient surfaces. RSC Adv 2015;5:45266–75.
[17] Lorenz MR, Novotny VJ, Deline VR. Lubricant migration in particulate magnetic recording media. IEEE Trans Magn 1991;27:5088–90.
[18] Cheng T, Zhao B, Chao J, Meeks SW, Velidandea V. The lubricant migration rate on the hard disk surface. Tribol Lett 2000;9:181–5.
[19] Liu D, Li K, Zhang S, Amann T, Zhang C, Yan X. Anti-spreading behavior of 1,3-diketone lubricating oil on steel surfaces. Tribol Int 2018;121:108–13.
[20] Grützmacher PG, Rosenkranz A, Szurdak A, Grüber M, Gachot C, Hirt G, et al. Multi-scale surface patterning – an approach to control friction and lubricant migration in lubricated systems. Ind Lubric Tribol 2019;71:1007–16.
[21] Radakovic DJ, Khonsari MM. Heat transfer in a thin-film flow in the presence of squeeze and shear thinning: application to piston rings. J Heat Tran 1997;119:249–57.
[22] Ma L, Luo J. Thin film lubrication in the past 20 years. Friction 2016;4:280–302.
[23] Li SY, Guo F, Li XM, Liu CL. Elastohydrodynamic lubrication with oil droplets. Tribol Lett 2017;65:162.
[24] Li XM, Guo F, Wong PL, Zhao Y. Regulation of lubricant supply by wettability gradient in rolling ehl contacts. Tribol Int 2018;120:565–74.
[25] Li X, Li J, Dong G. Bioinspired topological surface for directional oil lubrication. ACS Appl Mater Interfaces 2020;12:5113–9.
[26] Fote AA, Slade RA, Feuerstein S. Thermally induced migration of hydrocarbon oil. J Lubr Technol 1977;99:158–62.
[27] Kannel JW, Dufrane KF. Rolling element bearings in space. 20 th aerospace mechanisms symposium. 1986.
[28] Pochard M, Prat P, Sicre J, Vergne P. Thermocapillary migration of lubricants in space environment. International tribology conference- Austrib 941994.
[29] Dai QW, Huang W, Wang XL, Khonsari MM. Ringlike migration of a droplet propelled by an omnidirectional thermal gradient. Langmuir 2018;34:3806–12.
[30] Tadmor R. Line energy and the relation between advancing, receding, and young contact angles. Langmuir 2004;20:7659–64.
[31] Wasan DT, Nikolov AD, Brenner H. Droplets speeding on surfaces. Science 2001;291:605–6.
[32] Duhr S, Braun D. Why molecules move along a temperature gradient. Proc Natl Acad Sci Unit States Am 2006;103:19678–82.
[33] Lhost O, Platten JK. Large-scale convection induced by the soret effect. Phys Rev A 1989;40:6415–20.
[34] Platten JK. The soret effect: a review of recent experimental results. J Appl Mech 2006;73:5–15.
[35] Fusaro RL, Khonsari MM. Liquid lubrication for space applications. 1992. NASA TM-105198.
[36] Fusaro RL. Preventing spacecraft failures due to tribological problems. 2001. NASA/TM-2001-210806.
[37] Jones WR, Jansen MJ. Tribology for space applications. Proc Inst Mech Eng Part J J Eng Tribol 2008;222:997–1004.
[38] Zaretsky EV. Liquid lubrication in space. Tribol Int 1990;23:75–93.
[39] Dai QW, Huang W, Wang XL. Surface roughness and orientation effects on the thermo-capillary migration of a droplet of paraffin oil. Exp Therm Fluid Sci 2014;57:200–6.
[40] Ji YJ, Dai QW, Huang W, Wang XL. On the thermocapillary migration at the liquid and solid aspects. J Tribol 2019;141:091802-1–091802-7.
[41] Huang W, Wang XL. No migration of ionic liquid under temperature gradient. Colloids Surf, A 2016;497:167–70.
[42] Sartori P, Guglielmin E, Ferraro D, Filippi D, Zaltron A, Pierno M, et al. Motion of Newtonian drops deposited on liquid-impregnated surfaces induced by vertical vibrations. J Fluid Mech 2019;876. R4-1-11.
[43] Jing X, Guo Z. Durable lubricant-impregnated surfaces for water collection under extremely severe working conditions. Acs Appl Mater Inter 2019;11:35949–58.

[44] Ma Q, Wang W, Dong G. Facile fabrication of biomimetic liquid-infused slippery surface on carbon steel and its self-cleaning, anti-corrosion, anti-frosting and tribological properties. Colloids Surf, A 2019;577:17–26.
[45] Bjelobrk N, Girard H-L, Bengaluru Subramanyam S, Kwon H-M, Quéré D, Varanasi KK. Thermocapillary motion on lubricant-impregnated surfaces. Phys Rev Fluids 2016;1:063902.
[46] Yakhshi-Tafti E, Cho HJ, Kumar R. Droplet actuation on a liquid layer due to thermocapillary motion: shape effect. Appl Phys Lett 2010;96:264101.
[47] Yu DI, Kwak HJ, Doh SW, Ahn HS, Park HS, Kiyofumi M, et al. Dynamics of contact line depinning during droplet evaporation based on thermodynamics. Langmuir 2015;31:1950–7.
[48] Ouenzerfi S, Harmand S. Experimental droplet study of inverted marangoni effect of a binary liquid mixture on a nonuniform heated substrate. Langmuir 2016;32: 2378–88.
[49] Al-Sharafi A, Yilbas BS, Hassan G. Droplet on oil impregnated surface: temperature and velocity fields. Int J Therm Sci 2019;146. 106054.
[50] Vaikuntanathan V, Weigand B, Terzis A. Droplet mobilization at the walls of a microfluidic channel. Phys Fluids 2020;32:012004.
[51] Lu HW, Bottausci F, Fowler JD, Bertozzi AL, Meinhart C, Kim CJ. A study of ewod-driven droplets by piv investigation. Lab Chip 2008;8:456–61.
[52] Wang Z, Zhao Y-P. In situ observation of thermal marangoni convection on the surface of a sessile droplet by infrared thermal imaging. J Adhes Sci Technol 2012;26:2177–88.
[53] Pradhan TK, Panigrahi PK. Thermocapillary convection inside a stationary sessile water droplet on a horizontal surface with an imposed temperature gradient. Exp Fluid 2015;56:1–11.
[54] Li Y, Yoda M. Convection driven by a horizontal temperature gradient in a confined aqueous surfactant solution: the effect of noncondensables. Exp Fluid 2014;55:1663.
[55] Edward B. Motion of the liquid on the surface of leidenfrost droplets and the hairy ball theorem. Surface Innovations 2019;7:101–3.
[56] Zhao Y, Liu F, Chen C-H. Thermocapillary actuation of binary drops on solid surfaces. Appl Phys Lett 2011;99. 104101.
[57] Barton KD, Shankar Subramanian R. The migration of liquid drops in a vertical temperature gradient. J Colloid Interface Sci 1989;133:211–22.
[58] Schatz MF, Neitzel GP. Experiments on thermocapillary instabilities. Annu Rev Fluid Mech 2001;33:93–127.
[59] Burelbach JP, Bankoff SG, Davis SH. Steady thermocapillary flows of thin liquid layers. Ii. Experiment. Physics of Fluids A: Fluid Dynamics 1990;2:322.
[60] VanHook SJ, Schatz MF, Mccormick WD, Swift JB, Swinney HL. Long wavelength instability in surface tension driven benard convection. Phys Rev Lett 1995;75: 4397–400.
[61] Vanhook SJ, Schatz MF, Swift JB, Mccormick WD, Swinney HL. Long-wavelength surface-tension-driven benard convection: experiment and theory. J Fluid Mech 1997;345:45–78.
[62] Wakitani S. Experiments on instabilities of thermocapillary convection in shallow annular liquid layers. J Phys: Conf Ser 2007;64:012006.
[63] Frenkel M, Dombrovsky L, Multanen V, Danchuk V, Legchenkova I, Shoval S, et al. Self-propulsion of water-supported liquid marbles filled with sulfuric acid. J Phys Chem B 2018;122:7936–42.
[64] Gendelman O, Frenkel M, Binks BP, Bormashenko E. Cherenkov-like surface thermal waves emerging from self-propulsion of a liquid marble. J Phys Chem B 2020;124:695–9.
[65] Mattox DM, Smith HD, Wilcox WR, Subramanian RS. Thermal-gradient-inudced migration of bubbles in molten glass. J Am Ceram Soc 1982;65:437.
[66] Sen A, Davis SH. Steady thermocapillary flows in two-dimensional slots. J Fluid Mech 1982;121:163–86.
[67] Zhang JIN, Watson SJ, Wong H. Fluid flow and heat transfer in a dual-wet micro heat pipe. J Fluid Mech 2007;589:1–31.
[68] Mazouchi A, Homsy GM. Thermocapillary migration of long bubbles in polygonal tubes. I. Theory. Phys Fluids 2001;13:1594.
[69] Meyyappan M, Subramanian RS. Thermocapillary migration of a gas bubble in an arbitrary direction with respect to a plane surface. J Colloid Interface Sci 1987; 115:206–19.
[70] Barton KD, Shankar Subramanian R. Thermocapillary migration of a liquid drop normal to a plane surface. J Colloid Interface Sci 1990;137:170–82.
[71] Wang Y, Mauri R, Acrivos A. Thermocapillary migration of a bidisperse suspension of bubbles. J Fluid Mech 1994;261:47–64.
[72] Chen SH. Thermocapillary migration of a fluid sphere parallel to an insulated plane. Langmuir 1999;15:8618–26.
[73] Nierstrasz VA, Frens G. Marginal regeneration and the marangoni effect. J Colloid Interface Sci 1999;215:28–35.
[74] Gomba JM, Homsy GM. Regimes of thermocapillary migration of droplets under partial wetting conditions. J Fluid Mech 2010;647:125–42.
[75] Nierstrasz VA, Frens G. Marangoni flow driven instabilities and marginal regeneration. J Colloid Interface Sci 2001;234:162–7.
[76] Hu H, Larson RG. Analysis of the microfluid flow in an evaporating sessile droplet. Langmuir 2005;21:3963–71.
[77] Hu H, Larson RG. Analysis of the effects of marangoni stresses on the microflow in an evaporating sessile droplet. Langmuir 2005;21:3972–80.
[78] Tsoumpas Y, Dehaeck S, Rednikov A, Colinet P. Effect of marangoni flows on the shape of thin sessile droplets evaporating into air. Langmuir 2015;31:13334–40.
[79] Loulergue JC, Manneville P, Pomeau Y. Interface deflections induced by the marangoni effect: an application to infrared-visible image conversion. J Phys D: Appl Phys 1981;14:1967–77.
[80] Jasnow D, Viñals J. Coarse-grained description of thermo-capillary flow. Phys Fluids 1996;8:660–9.
[81] Karapetsas G, Sahu KC, Sefiane K, Matar OK. Thermocapillary-driven motion of a sessile drop: effect of non-monotonic dependence of surface tension on temperature. Langmuir 2014;30:4310–21.
[82] Sumner LBS. Lubrication analysis of thermocapillary-induced nonwetting. Phys Fluids 2003;15:2923–33.
[83] Brochard F. Motions of droplets on solid surfaces induced by chemical or thermal gradients. Langmuir 1989;5:432–8.
[84] Chen JZ, Troian SM, Darhuber AA, Wagner S. Effect of contact angle hysteresis on thermocapillary droplet actuation. J Appl Phys 2005;97:014906.
[85] Dai QW, Huang W, Wang XL. Contact angle hysteresis effect on the thermocapillary migration of liquid droplets. J Colloid Interface Sci 2018;515: 32–8.
[86] Karapetsas G, Chamakos NT, Papathanasiou AG. Thermocapillary droplet actuation: effect of solid structure and wettability. Langmuir 2017;33:10838–50.
[87] Dai QW, Ji YJ, Huang W, Wang XL. On the thermocapillary migration on radially microgrooved surfaces. Langmuir 2019;35:9169–76.
[88] Wang R, Bai S. Modeling and experimental analysis of thermocapillary effect on laser grooved surfaces at high temperature. Appl Surf Sci 2019;465:41–7.
[89] Hu K-X, Yan C-Y, Chen Q-S. Instability of thermocapillary–buoyancy convection in droplet migration. Phys Fluids 2019;31. 122101.
[90] Brzoska JB, Brochard-Wyart F, Rondelez F. Motions of droplets on hydrophobic model surfaces induced by thermal gradients. Langmuir 1993;9:2220–4.
[91] Smith MK. Thermocapillary migration of a two-dimensional liquid droplet on a solid surface. J Fluid Mech 1995;294:209–30.
[92] Smith M, Davis SH. Instabilities of dynamic thermocapillary liquid layers. Part 1. Convective instabilities. J Fluid Mech 1983;132:119–44.
[93] Davis SH. Thermocapillary instabilities. Annu Rev Fluid Mech 1987;19:403–35.
[94] Anderson DM, Davis SH. The spreading of volatile liquid droplets on heated surfaces. Phys Fluids 1995;7:248.
[95] Ehrhard P, Davis SH. Non-isothermal spreading of liquid drops on horizontal plates. J Fluid Mech 1991;229:365–88.
[96] Daniel S, Chaudhury MK, de Gennes PG. Vibration-actuated drop motion on surfaces for batch microfluidic processes. Langmuir 2005;21:4240–8.
[97] Mettu S, Chaudhury MK. Motion of drops on a surface induced by thermal gradient and vibration. Langmuir 2008;24:10833–7.
[98] Mac Intyre JR, Gomba JM, Perazzo CA, Correa PG, Sellier M. Thermocapillary migration of droplets under molecular and gravitational forces. J Fluid Mech 2018;847:1–27.
[99] Ford ML, Nadim A. Thermocapillary migration of an attached drop on a solid surface. Phys Fluids 1994;6:3183–5.
[100] Hadland PH, Balasubramaniam R, Wozniak G, Subramanian RS. Thermocapillary migration of bubbles and drops at moderate to large marangoni number and moderate Reynolds number in reduced gravity. Exp Fluid 1999;26:240–8.
[101] Balasubramaniam R, Subramanian RS. The migration of a drop in a uniform temperature gradient at large marangoni numbers. Phys Fluids 2000;12:733–43.
[102] Balasubramaniam R, Subramanian RS. Thermocapillary migration of a drop: an exact solution with Newtonian interfacial rheology and stretching/shrinkage of interfacial area elements for small marangoni numbers. Ann N Y Acad Sci 2004; 1027:303–10.
[103] Mamalis D, Koutsos V, Sefiane K. On the motion of a sessile drop on an incline: effect of non-monotonic thermocapillary stresses. Appl Phys Lett 2016;109. 231601.
[104] Karapetsas G, Sahu KC, Matar OK. Effect of contact line dynamics on the thermocapillary motion of a droplet on an inclined plate. Langmuir 2013;29: 8892–906.
[105] Dai QW, Khonsari MM, Shen C, Huang W, Wang XL. On the migration of a droplet on an incline. J Colloid Interface Sci 2017;494:8–14.
[106] Pratap V, Moumen N, Subramanian RS. Thermocapillary motion of a liquid drop on a horizontal solid surface. Langmuir 2008;24:5185–93.
[107] Greenspan HP. On the motion of a small viscous droplet that wets a surface. J Fluid Mech 1978;84:125–43.
[108] De Gennes P. Wetting: statics and dynamics. Rev Mod Phys 1985;57:827–63.
[109] Herminghaus S, Brinkmann M, Seemann R. Wetting and dewetting of complex surface geometries. Annu Rev Mater Res 2008;38:101–21.
[110] Dardelle G, Erni P. Three-phase interactions and interfacial transport phenomena in coacervate/oil/water systems. Adv Colloid Interface Sci 2014;206:79–91.
[111] Tadmor R. Line energy, line tension and drop size. Surf Sci 2008;602:L108–11.
[112] Tadmor R, Bahadur P, Leh A, N'Guessan HE, Jaini R, Dang L. Measurement of lateral adhesion forces at the interface between a liquid drop and a substrate. Phys Rev Lett 2009;103:266101.
[113] Tadmor R. Approaches in wetting phenomena. Soft Matter 2011;7:1577–80.
[114] Le Grand N, Daerr A, Limat L. Shape and motion of drops sliding down an inclined plane. J Fluid Mech 2005;541:293–315.
[115] Extrand CW, Kumagai Y. Liquid drops on an inclined plane: the relation between contact angles, drop shape, and retentive force. J Colloid Interface Sci 1995;170: 515–21.
[116] ElSherbini AI, Jacobi AM. Critical contact angles for liquid drops on inclined surfaces. Prog Colloid Polym Sci 2004;128:57–62.
[117] Anderson JL. Droplet interactions in thermocapillary motion. Int J Multiphas Flow 1985;11:813–24.
[118] Wu X, Phan-Thien N, Fan X-J, Ng TY. A molecular dynamics study of drop spreading on a solid surface. Phys Fluids 2003;15:1357–62.
[119] Grigoriev RO. Chaotic mixing in thermocapillary-driven microdroplets. Phys Fluids 2005;17:033601.

[120] Vainchtein DL, Widloski J, Grigoriev RO. Mixing properties of steady flow in thermocapillary driven droplets. Phys Fluids 2007;19:067102.
[121] He Y, Wang Y, Li Q. Lattice Boltzmann method: theory and application. Beijing: Science Press; 2008.
[122] Guo Z, Zheng C. Theory and application of lattice Boltzmann method. Beijing: Science Press; 2008.
[123] Greco EF, Grigoriev RO. Thermocapillary migration of interfacial droplets. Phys Fluids 2009;21:042105.
[124] Wang T, Li W, Liu L, Chen H, Wang Y, Zhang J, et al. The mechanism for the motion of nanoscale water droplet induced by wetting gradient: a molecular dynamic study. Comput Mater Sci 2015;105:39–46.
[125] Cheng J, Wang G, Zhang Y, Pi P, Xu S. Enhancement of capillary and thermal performance of grooved copper heat pipe by gradient wettability surface. Int J Heat Mass Tran 2017;107:586–91.
[126] Ding Z, Wong TN. Three-dimensional dynamics of thin liquid films on vertical cylinders with marangoni effect. Phys Fluids 2017;29:011701.
[127] Haj-Hariri H, Shi Q, Borhan A. Thermocapillary motion of deformable drops at finite Reynolds and marangoni numbers. Phys Fluids 1997;9:845.
[128] Herrmann M, Lopez JM, Brady P, Raessi M. Thermocapillary motion of deformable drops and bubbles. Proceedings of the summer program. Center for Turbulence Research; 2008. p. 155–70.
[129] Sui Y. Moving towards the cold region or the hot region? Thermocapillary migration of a droplet attached on a horizontal substrate. Phys Fluids 2014;26: 092102.
[130] Nguyen H-B, Chen J-C. A numerical study of thermocapillary migration of a small liquid droplet on a horizontal solid surface. Phys Fluids 2010;22:062102.
[131] Le T-L, Chen J-C, Shen B-C, Hwu F-S, Nguyen H-B. Numerical investigation of the thermocapillary actuation behavior of a droplet in a microchannel. Int J Heat Mass Tran 2015;83:721–30.
[132] Sun T, Jiang C, Ding J, Yuan N. Thermocapillary migration mechanism of molten silicon droplets on horizontal solid surfaces. Friction 2017;3:1–13.
[133] Tseng Y-T, Tseng F-G, Chen Y-F, Chieng C-C. Fundamental studies on micro-droplet movement by marangoni and capillary effects. Sens Actuator A-Phys. 2004;114:292–301.
[134] Alhendal Y, Turan A, Aly WIA. Vof simulation of marangoni flow of gas bubbles in 2d-axisymmetric column. Procedia Comput Sci 2010;1:673–80.
[135] Alhendal Y, Turan A. Thermocapillary bubble dynamics in a 2d axis swirl domain. Heat Mass Tran 2014;51:529–42.
[136] Samareh B, Mostaghimi J, Moreau C. Thermocapillary migration of a deformable droplet. Int J Heat Mass Tran 2014;73:616–26.
[137] Chaudhury K, Chakraborty S. Spreading of a droplet over a nonisothermal substrate: multiple scaling regimes. Langmuir 2015;31:4169–75.
[138] Ma C, Bothe D. Direct numerical simulation of thermocapillary flow based on the volume of fluid method. Int J Multiphas Flow 2011;37:1045–58.
[139] Fath A, Bothe D. Direct numerical simulations of thermocapillary migration of a droplet attached to a solid wall. Int J Multiphas Flow 2015;77:209–21.
[140] Yin Z, Chang L, Hu W, Li Q, Wang H. Numerical simulations on thermocapillary migrations of nondeformable droplets with large marangoni numbers. Phys Fluids 2012;24:092101.
[141] Chen X, Wang X, Chen PG, Liu Q. Thermal effects of substrate on marangoni flow in droplet evaporation: response surface and sensitivity analysis. Int J Heat Mass Tran 2017;113:354–65.
[142] Le T-L, Chen J-C, Nguyen H-B. Numerical study of the thermocapillary droplet migration in a microchannel under a blocking effect from the heated upper wall. Appl Therm Eng 2017;122:820–30.
[143] Li C, Zhao D, Wen J, Lu X. Numerical investigation of wafer drying induced by the thermal marangoni effect. Int J Heat Mass Tran 2019;132:689–98.
[144] Nas S, Tryggvason G. Thermocapillary interaction of two bubbles or drops. Int J Multiphas Flow 2003;29:1117–35.
[145] Yin Z, Gao P, Hu W, Chang L. Thermocapillary migration of nondeformable drops. Phys Fluids 2008;20:082101.
[146] Wu Z-B. Terminal states of thermocapillary migration of a planar droplet at moderate and large marangoni numbers. Int J Heat Mass Tran 2017;105:704–11.
[147] Liu H, Zhang Y. Modelling thermocapillary migration of a microfluidic droplet on a solid surface. J Comput Phys 2015;280:37–53.
[148] Liu H, Zhang Y, Valocchi AJ. Modeling and simulation of thermocapillary flows using lattice Boltzmann method. J Comput Phys 2012;231:4433–53.
[149] Liu H, Valocchi AJ, Zhang Y, Kang Q. Lattice Boltzmann phase-field modeling of thermocapillary flows in a confined microchannel. J Comput Phys 2014;256: 334–56.
[150] Liu H, Wu L, Ba Y, Xi G. A lattice Boltzmann method for axisymmetric thermocapillary flows. Int J Heat Mass Tran 2017;104:337–50.
[151] Liu C, Lv Y, Li Z. Fluid transport in nanochannels induced by temperature gradients. J Chem Phys 2012;136. 114506.
[152] Yd S, Maroo SC. Origin of surface-driven passive liquid flows. Langmuir 2016;32: 8593–7.
[153] B C, SHP D, Chakraborty S. Mimicking wettability alterations using temperature gradients for water nanodroplets. Nanoscale 2017;9:12509–15.
[154] Foroutan M, Fatemi SM, Esmaeilian F, Naeini VF, Baniassadi M. Contact angle hysteresis and motion behaviors of a water nano-droplet on suspended graphene under temperature gradient. Phys Fluids 2018;30:052101.
[155] Wang J, Zhang Y, Wang X, Maginn EJ. Layer-based thermal migration of an ionic liquid nano-droplet on a graphene surface: a molecular dynamics study. Mol Simulat 2020;46:829–36.
[156] Ratoi M, Anghel V, Bovington C, Spikes HA. Mechanisms of oiliness additives. Tribol Int 2000;33:241–7.
[157] Spikes H. The history and mechanisms of zddp. Tribol Lett 2004;17:469–89.
[158] Mosey NJ, Muser MH, Woo TK. Molecular mechanisms for the functionality of lubricant additives. Science 2005;307:1612–5.
[159] Stone HA, Lealz lG. The effects of surfactants on drop deformation and breakup. J Fluid Mech 1990;220:161–86.
[160] He S, Ketterson JB. Surfactant-driven spreading of a liquid on a vertical surface. Phys Fluids 1995;7:2640–7.
[161] Bahr M, Tiberg F, Zhmud BV. Spreading dynamics of surfactant solutions. Langmuir 1999:7069–75.
[162] Clay MA, Miksis MJ. Effects of surfactant on droplet spreading. Phys Fluids 2004; 16:3070–8.
[163] Theodorakis PE, Müller EA, Craster RV, Matar OK. Modelling the superspreading of surfactant-laden droplets with computer simulation. Soft Matter 2015;48: 9254–61.
[164] Marin A, Liepelt R, Rossi M, Kahler CJ. Surfactant-driven flow transitions in evaporating droplets. Soft Matter 2016;12:1593–600.
[165] Wang X, Venzmer J, Bonaccurso E. Surfactant-enhanced spreading of sessile water drops on polypropylene surfaces. Langmuir 2016;32:8322–8.
[166] Chen YS, Lu yL, Yang yM, Maa jR. Surfactant effects on the motion of a droplet in thermocapillary migration. Int J Multiphas Flow 1996;23:325–35.
[167] Das S, Mandal S, Som SK, Chakraborty S. Migration of a surfactant-laden droplet in non-isothermal Poiseuille flow. Phys Fluids 2017;29:012002.
[168] Dai QW, Huang W, Wang XL. Insights into the influence of additives on the thermal gradient induced migration of lubricant. Lubric Sci 2017;29:17–29.
[169] Tabor RF, Eastoe J, Dowding PJ. A two-step model for surfactant adsorption at solid surfaces. J Colloid Interface Sci 2010;346:424–8.
[170] Fote AA, Slade RA, Feuerstein S. The prevention of lubricant migration in spacecraft. Wear 1978;51:67–75.
[171] Klien S, Surberg CH, Stehr W. Temperature diven lubricant migration on tribological surface. In: Proceedings - ECOTRIB 2007, Ljubljana, Slovenia; 2007. p. 637–47.
[172] Wang R, Li S, Bai S. Thermodynamic spreading behaviors of oil on rough surfaces of stainless steel 316l. Appl Surf Sci 2019;478:1046–55.
[173] Dai QW, Li M, Khonsari MM, Huang W, Wang XL. The thermocapillary migration on rough surfaces. Lubric Sci 2019;31:163–70.
[174] Wang DA, Wang XL, Liu XJ, Zhou F. Engineering a titanium surface with controllable oleophobicity and switchable oil adhesion. J Phys Chem C 2010;114: 9938–44.
[175] Dai QW, Huang W, Wang XL. A surface texture design to obstruct the liquid migration induced by omnidirectional thermal gradients. Langmuir 2015;31: 10154–60.
[176] Dai QW, Huang W, Wang XL. Micro-grooves design to modify the thermo-capillary migration of paraffin oil. Meccanica 2017;52:171–81.
[177] Long J, Weng Q, Hong W, Cao Z, Zhou P, Xie X. Fast water flow in laser micromachined microgrooves with nonuniform surface wettability. Exp Therm Fluid Sci 2019;103:9–17.
[178] Zhang Y, Jiao Y, Chen C, Zhu S, Li C, Li J, et al. Reversible tuning between isotropic and anisotropic sliding by one-direction mechanical stretching on microgrooved slippery surfaces. Langmuir 2019;35:10625–30.
[179] Zhang P, Liu H, Meng J, Yang G, Liu X, Wang S, et al. Grooved organogel surfaces towards anisotropic sliding of water droplets. Adv Mater 2014;26:3131–5.
[180] Grützmacher PG, Rosenkranz A, Szurdak A, Gachot C, Hirt G, Mücklich F. Lubricant migration on stainless steel induced by bio-inspired multi-scale surface patterns. Mater Des 2018;150:55–63.
[181] Grützmacher PG, Rosenkranz A, Gachot C. How to guide lubricants – tailored laser surface patterns on stainless steel. Appl Surf Sci 2016;370:59–66.
[182] Bliznyuk O, Jansen HP, Kooij ES, Zandvliet HJ, Poelsema B. Smart design of stripe-patterned gradient surfaces to control droplet motion. Langmuir 2011;27: 11238–45.
[183] Yang J-T, Yang Z-H, Chen C-Y, Yao D-J. Conversion of surface energy and manipulation of a single droplet across micropatterned surfaces. Langmuir 2008; 24:9889–97.
[184] Lai Y-H, Yang J-T, Shieh D-B. A microchip fabricated with a vapor-diffusion self-assembled-monolayer method to transport droplets across superhydrophobic to hydrophilic surfaces. Lab Chip 2009;10:499–504.
[185] Lv CJ, Hao PF. Driving droplet by scale effect on microstructured hydrophobic surfaces. Langmuir 2012;28:16958–65.
[186] Kita Y, Mackenzie Dover C, Askounis A, Takata Y, Sefiane K. Drop mobility on superhydrophobic microstructured surfaces with wettability contrasts. Soft Matter 2018;14:9418–24.
[187] Sommers AD, Brest TJ, Eid KF. Topography-based surface tension gradients to facilitate water droplet movement on laser-etched copper substrates. Langmuir 2013;29:12043–50.
[188] Li J, Tian XL, Perros AP, Franssila S, Jokinen V. Self-propelling and positioning of droplets using continuous topography gradient surface. Adv Mater Inter 2014;vol. 1:1400001.
[189] Zamuruyev KO, Bardaweel HK, Carron CJ, Kenyon NJ, Brand O, Delplanque JP, et al. Continuous droplet removal upon dropwise condensation of humid air on a hydrophobic micropatterned surface. Langmuir 2014;30:10133–42.
[190] Bliznyuk O, Seddon JRT, Veligura V, Kooij ES, Zandvliet HJW, Poelsema B. Directional liquid spreading over chemically defined radial wettability gradients. Acs Appl Mater Inter 2012;4:4141–8.
[191] Dhiman S, Jayaprakash KS, Iqbal R, Sen AK. Self-transport and manipulation of aqueous droplets on oil-submerged diverging groove. Langmuir 2018;34: 12359–68.

[192] Zhang Z, Guo X, Tang H, Ding J, Zheng YG, Li S. Unidirectional self-driving liquid droplet transport on a monolayer graphene-covered textured substrate. ACS Appl Mater Interfaces 2019;11:28562–70.
[193] Qi L, Niu Y, Ruck C, Zhao Y. Mechanical-activated digital microfluidics with gradient surface wettability. Lab Chip 2019;19:223–32.
[194] Nakashima Y, Nakanishi Y, Yasuda T. Automatic droplet transportation on a plastic microfluidic device having wettability gradient surface. Rev Sci Instrum 2015;86:015001.
[195] Alheshibri MH, Rogers NG, Sommers AD, Eid KF. Spontaneous movement of water droplets on patterned cu and al surfaces with wedge-shaped gradients. Appl Phys Lett 2013;102:174103.
[196] Li J, Zhou X, Zhang Y, Hao C, Zhao F, Li M, et al. Rectification of mobile leidenfrost droplets by planar ratchets. Small 2019:e1901751.
[197] Dai QW, Ji YJ, Chong ZJ, Huang W, Wang XL. Manipulating thermocapillary migration via superoleophobic surfaces with wedge shaped superoleophilic grooves. J Colloid Interface Sci 2019;557:837–44.
[198] Liu M, Yao Y, Yang Y, Peng Z, Chen S. Directional transport behavior of droplets on wedge-shaped functional surfaces. J Phys Chem C 2019;123:12736–43.
[199] Zheng YF, Cheng J, Zhou CL, Xing HT, Wen XF, Pi PH, et al. Droplet motion on a shape gradient surface. Langmuir 2017;33:4172–7.
[200] Huang S, Song J, Lu Y, Chen F, Zheng H, Yang X, et al. Underwater spontaneous pumpless transportation of nonpolar organic liquids on extreme wettability patterns. ACS Appl Mater Interfaces 2016;8:2942–9.
[201] Wang M, Liu Q, Zhang H, Wang C, Wang L, Xiang B, et al. Laser direct writing of tree-shaped hierarchical cones on a superhydrophobic film for high-efficiency water collection. ACS Appl Mater Interfaces 2017;9:29248–54.
[202] Yao Z, Bowick MJ. Self-propulsion of droplets by spatially-varying surface topography. Soft Matter 2012;8:1142–5.
[203] Liu C, Sun J, Li J, Xiang C, Che L, Wang Z, et al. Long-range spontaneous droplet self-propulsion on wettability gradient surfaces. Sci Rep 2017;7:7552.
[204] Wang L, Zhan S, Qin P, Tang S, Yang J, Yu W, et al. The investigation of de-icing and uni-directional droplet driven on a soft liquid-metal chip controlled through electrical current. J Taiwan Inst Chem Eng 2020;106:191–7.
[205] Kang SM, Lee C, Kim HN, Lee BJ, Lee JE, Kwak MK, et al. Directional oil sliding surfaces with hierarchical anisotropic groove microstructures. Adv Mater 2013;25:5756–61.
[206] Yan X, Jin Y, Chen X, Zhang C, Hao C, Wang Z. Nature-inspired surface topography: design and function. Sci China Phys Mech Astron 2019;63:224601.
[207] Zhang W, Ding W, Fernandino M, Dorao CA. Water-repellent surfaces consisting of nanowires on micropyramidal structures. ACS Appl. Nano Mater. 2019;2:7696–704.
[208] Wang Y, Cui C, Qi B, Wei J, Zhang Y. Study of droplet self-migration on silicon surface with radial micro-fin structures. Exp Therm Fluid Sci 2020;114:110075.
[209] Zhang PF, Chen HW, Li L, Liu HL, Liu G, Zhang LW, et al. Bioinspired smart peristome surface for temperature-controlled unidirectional water spreading. Appl Mater Interfaces 2017;9:5645–52.
[210] Li J, Zhou X, Li J, Che L, Yao J, McHale G, et al. Topological liquid diode. Sci Adv 2017;3:eaao3530.
[211] Dai X, Sun N, Nielsen SO, Stogin BB, Wang J, Yang S, et al. Hydrophilic directional slippery rough surfaces for water harvesting. Sci Adv 2018;4:eaaq0919.
[212] Chen H, Zhang P, Zhang L, Liu H, Jiang Y, Zhang D, et al. Continuous directional water transport on the peristome surface of nepenthes alata. Nature 2016;532:85–9.
[213] Liu C, Legchenkova I, Han L, Ge W, Lv C, Feng S, et al. Directional droplet transport mediated by circular groove arrays. Part i: experimental findings. Langmuir 2020;36:9608–15.
[214] Dai QW, Qiu ZH, Chong ZJ, Huang W, Wang XL. Propelling liquids on superhydrophobic surfaces with superhydrophilic diverging grooves. Surface Innovations 2020;8:158–64.
[215] Roberts EW, Todd MJ. Space and vacuum tribology. Wear 1990;136:157–67.
[216] Chaudhury MK, Whitesides GM. How to make water run uphill. Science 1992;256:1539–41.
[217] Tadmor R. Drops that pull themselves up. Surf Sci 2014;628:17–20.
[218] Bormashenko E. Wetting of flat gradient surfaces. J Colloid Interface Sci 2018;515:264–7.
[219] Morgenthaler S, Zink C, Spencer ND. Surface-chemical and -morphological gradients. Soft Matter 2008;4:419–34.
[220] Chowdhury IU, Mahapatra PS, Sen AK. Self-driven droplet transport: effect of wettability gradient and confinement. Phys Fluids 2019;31:042111.
[221] Daniel S, Chaudhury MK, Chen JC. Fast drop movements resulting from the phase change on a gradient surface. Science 2001;291:633–6.
[222] Naik VV, Städler R, Spencer ND. Effect of leaving group on the structures of alkylsilane sams. Langmuir 2014;30:14824–31.
[223] Faustini M, Ceratti DR, Louis B, Boudot M, Albouy P-A, Boissière C, et al. Engineering functionality gradients by dip coating process in acceleration mode. Acs Appl Mater Inter 2014;6:17102–10.
[224] Miles J, Schlenker S, Ko Y, Patil R, Rao BM, Genzer J. Design and fabrication of wettability gradients with tunable profiles through degrafting organosilane layers from silica surfaces by tetrabutylammonium fluoride. Langmuir 2017;33:14556–64.
[225] Zhao M-X, Li J, Gao X. Gradient coating of polydopamine via cdr. Langmuir 2017;33:6727–31.
[226] Xing Y, Shang W, Wang Q, Feng S, Hou Y, Zheng Y. Integrative bioinspired surface with wettable patterns and gradient for enhancement of fog collection. ACS Appl Mater Interfaces 2019;11:10951–8.
[227] Ashraf KM, Wang C, Nair SS, Wynne KJ, Higgins DA, Collinson MM. Base layer influence on protonated aminosilane gradient wettability. Langmuir 2017;33:4207–15.
[228] Morgenthaler S, Lee S, Zürcher S, Spencer ND. A simple, reproducible approach to the preparation of surface-chemical gradients. Langmuir 2003;19:10459–62.
[229] Liao Q, Wang H, Zhu X, Li M. Liquid droplet movement on horizontal surface with gradient surface energy. Sci China Ser E: Technol Sci 2006;49:733–41.
[230] Loos K, Kennedy SB, Eidelman N, Tai Y, Zharnikov M, Amis EJ, et al. Combinatorial approach to study enzyme/surface interactions. Langmuir 2005;21:5237–41.
[231] Aono Y, Hirata A, Tokura H. Non-textured laser modification of silica glass surface: wettability control and flow channel formation. Appl Surf Sci 2016;371:530–7.
[232] Karapanagiotis I, Manoudis PN, Zurba A, Lampakis D. From hydrophobic to superhydrophobic and superhydrophilic siloxanes by thermal treatment. Langmuir 2014;30:13235–43.
[233] Song C, Kim K, Lee K, Pak HK. Thermochemical control of oil droplet motion on a solid substrate. Appl Phys Lett 2008;93:084102.
[234] Neuhaus S, Spencer ND, Padeste C. Anisotropic wetting of microstructured surfaces as a function of surface chemistry. ACS Appl Mater Interfaces 2012;4:123–30.
[235] Singh MK, Ilg P, Espinosa-Marzal RM, Kröger M, Spencer ND. Polymer brushes under shear: molecular dynamics simulations compared to experiments. Langmuir 2015;31:4798–805.
[236] Ramakrishna SN, Espinosa-Marzal RM, Naik VV, Nalam PC, Spencer ND. Adhesion and friction properties of polymer brushes on rough surfaces: a gradient approach. Langmuir 2013;29:15251–9.
[237] Dübner M, Spencer ND, Padeste C. Light-responsive polymer surfaces via postpolymerization modification of grafted polymer-brush structures. Langmuir 2014;30:14971–81.
[238] Li A, Ramakrishna SN, Schwarz T, Benetti EM, Spencer ND. Tuning surface mechanical properties by amplified polyelectrolyte self-assembly: where "grafting-from" meets "grafting-to". Acs Appl Mater Inter 2013;5:4913–20.
[239] Kakade B, Mehta R, Durge A, Kulkarni S, Pillai V. Electric field induced, superhydrophobic to superhydrophilic switching in multiwalled carbon nanotube papers. Nano Lett 2008;8:2693–6.
[240] Annapragada SR, Dash S, Garimella SV, Murthy JY. Dynamics of droplet motion under electrowetting actuation. Langmuir 2011;27:8198–204.
[241] Zhang G, Walker M, Unwin PR. Low-voltage voltammetric electrowetting of graphite surfaces by ion intercalation/deintercalation. Langmuir 2016;32:7476–84.
[242] Guo T, Che P, Heng L, Fan L, Jiang L. Anisotropic slippery surfaces: electric-driven smart control of a drop's slide. Adv Mater 2016;28.
[243] Tian D, He L, Zhang N, Zheng X, Dou Y, Zhang X, et al. Electric field and gradient microstructure for cooperative driving of directional motion of underwater oil droplets. Adv Funct Mater 2016;26:7986–92.
[244] Cao Q, Li L, Huang F, Zuo C. Ion-specific effects on the elongation dynamics of a nanosized water droplet in applied electric fields. Langmuir 2017;33:428–37.
[245] Dai H, Gao C, Sun J, Li C, Li N, Wu L, et al. Controllable high-speed electrostatic manipulation of water droplets on a superhydrophobic surface. Adv Mater 2019;31:e1905449.
[246] Xu W, Xu J, Li X, Tian Y, Choi CH, Yang EH. Lateral actuation of an organic droplet on conjugated polymer electrodes via imbalanced interfacial tensions. Soft Matter 2016;12:6902–9.
[247] Frenkel M, Vilk A, Legchenkova I, Shoval S, Bormashenko E. Mini-generator of electrical power exploiting the marangoni flow inspired self-propulsion. ACS Omega 2019;4:15265–8.
[248] Borcia R, Borcia ID, Bestehorn M. Can vibrations control drop motion? Langmuir 2014;30:14113–7.
[249] Sartori P, Quagliati D, Varagnolo S, Pierno M, Mistura G, Magaletti F, et al. Drop motion induced by vertical vibrations. New J Phys 2015;17:113017.
[250] Ichimura K, Oh S-K, Nakagawa M. Light-driven motion of liquids on a photoresponsive surface. Science 2000;288:1624–6.
[251] Telitel S, Telitel S, Bosson J, Lalevee J, Clement JL, Godfroy M, et al. Uv-induced micropatterning of complex functional surfaces by photopolymerization controlled by alkoxyamines. Langmuir 2015;31:10026–36.
[252] Feldmann D, Maduar SR, Santer M, Lomadze N, Vinogradova OI, Santer S. Manipulation of small particles at solid liquid interface: light driven diffusioosmosis. Sci Rep 2016;6:36443.
[253] Sumino Y, Magome N, Hamada T, Yoshikawa K. Self-running droplet: emergence of regular motion from nonequilibrium noise. Phys Rev Lett 2005;94. 068301-1.
[254] Rezk AR, Manor O, Friend JR, Yeo LY. Unique fingering instabilities and soliton-like wave propagation in thin acoustowetting films. Nat Commun 2012;3:1167.
[255] Ody T, Panth M, Sommers AD, Eid KF. Controlling the motion of ferrofluid droplets using surface tension gradients and magnetoviscous pinning. Langmuir 2016;32:6967–76.
[256] Ke HJ, Huang W, Wang XL. Controlling lubricant migration using ferrofluids. Tribol Int 2016;93:318–23.
[257] Dai QW, Huang W, Wang JQ, Wang XL. The thermal capillary migration properties and controlling technique of ferrofluids. Proc IMechE Part J: Eng Tribiol 2017;231:1441–9.
[258] Al-Azawi A, Latikka M, Jokinen V, Franssila S, Ras RHA. Friction and wetting transitions of magnetic droplets on micropillared superhydrophobic surfaces. Small 2017;13. 1700860-n/a.

[259] Lee JB, Derome D, Dolatabadi A, Carmeliet J. Energy budget of liquid drop impact at maximum spreading: numerical simulations and experiments. Langmuir 2016; 32:1279–88.
[260] Russell AC, Hsieh WL, Chen KC, Heikenfeld J. Experimental and numerical insights into isotropic spreading and deterministic dewetting of dielectrowetted films. Langmuir 2014;31:637–42.
[261] Daniel S, Chaudhury MK. Rectified motion of liquid drops on gradient surfaces induced by vibration. Langmuir 2002;18:3404–7.
[262] Chong ZJ, Dai QW, Huang W, Wang XL. Investigations on the thermocapillary migration of liquid lubricants at different interfaces. Tribol Lett 2020;68:59.
[263] Dai QW, Chong ZJ, Huang W, Wang XL. Migration of liquid bridges at the interface of spheres and plates with an imposed thermal gradient. Langmuir 2020; 36:6268–76.
[264] Castrejón-Pita JR, Muñoz-Sánchez BN, Hutchings IM, Castrejón-Pita AA. Droplet impact onto moving liquids. J Fluid Mech 2016;809:716–25.
[265] Ke HJ, Huang W, Wang XL. Insights into the effect of thermocapillary migration of droplet on lubrication. Proc Inst Mech Eng Part J J Eng Tribol 2016;230: 583–90.
[266] Wang X, Kato K, Adachi K. Running-in effect on the load-carrying capacity of a water-lubricated sic thrust bearing. Proc Inst Mech Eng Part J J Eng Tribol 2005; 219:117–24.
[267] Dai QW, Li SY, Wang XY, Huang W, Wang XL. Surface texturing of different sealing materials and their lubrication and sealing performances. China Surf Eng 2019;32:21–9.
[268] Derjaguin BV, Churaev NV. Structural component of disjoining pressure. J Colloid Interface Sci 1974;49:249–55.
[269] Mate CM, Carpick RW. Tribology on the small scale. Oxford University Press; 2008.